UNIVERSITY OF MINNESOTA
ST. ANTHONY FALLS HYDRAULIC LABORATORY

Project Report No. 114

Shear and Diffusion in a Large Boundary Layer Injected with Polymer Solution

by
JOSEPH M. WETZEL
and
JOHN F. RIPKEN

This research was sponsored by the Department of Hydromechanics of the Naval Ship Research and Development Center under Naval Ship Systems Command Subproject SF 35.421.003, Task 1710 Contract Nonr 710(71).

FEBRUARY 1970

MINNEAPOLIS, MINNESOTA

CONTENTS

LIST OF ILLUSTRATIONS

Figure

LIST OF SYMBOLS

c - average concentration at location y

c_H - concentration for homogeneous solution

c_i - concentration of injected solution

c_o - average concentration at boundary

C_D - total drag coefficient

C_f - local drag coefficient

d - water depth

D - pipe diameter

E_B - time-averaged bridge voltage

$F(n)$ - normalized power spectral density

k - mixing length constant

m - exponent of power law velocity distribution

n - frequency

N_o - number of positive-going zero crossings per unit time in turbulent fluctuation

q_i - injection discharge per unit width

R - pipe radius

Re - Reynolds number

u - average local velocity

u_* - shear velocity

U - free stream velocity

U_c - velocity at pipe centerline

V - average velocity in pipe

x - distance from injection slot to measuring station

x_1 - distance from orifice bulkhead to measuring station

x' - distance from origin of boundary layer to measuring station

y - vertical distance from boundary

δ - boundary layer thickness

δ_* - displacement thickness

θ - momentum thickness

λ - value of y where $c = 0.5\, c_o$

ν - kinematic viscosity

ρ - water density

τ_o - wall shear stress

Subscripts:

p - polymer

w - water

ABSTRACT

Experimental studies involving velocity profile measurements and polymer diffusion measurements were made in a plane boundary layer with length varying up to 40 feet, thickness varying up to 15 inches, and Reynolds number varying up to 8×10^7. Aqueous solutions of Polyox WSR-301 of 250 to 2000 ppm were injected tangentially at the boundary near the origin of a boundary layer having a stream velocity of 18 fps.

Diffusion of the polymer from the boundary up into the boundary layer was evaluated from profiles made by sampling with withdrawal tubes located at various stations along the flow axis. A fluorescent marker dye was used for the evaluation.

Velocity measurements served to define the profile and permitted profile extrapolation to the boundary for boundary shear evaluations.

The maximum drag reduction of 35 per cent over a 40-foot boundary length exposed to $V = 18$ fps occurred with an injection of 0.004 lb/sec of polymer per foot width, which resulted in a downstream wall concentration of about 30 ppm.

A flush-mounted hot-film sensor was calibrated for both water and polymer flows in a gravity-flow pipe facility. The calibration curve was influenced by the addition of polymer. Measurements of the zero crossings and frequency spectra of the turbulent fluctuations, as well as velocity profiles, were made for various polymer concentrations in the commercially rough pipe. Zero crossings were found to correlate with the square root of the wall shear stress.

SHEAR AND DIFFUSION IN A LARGE BOUNDARY LAYER INJECTED WITH POLYMER CONCENTRATE

I. INTRODUCTION

The concept of drag reduction by the addition of certain high-molecular-weight polymers to turbulent flow has been well demonstrated in the laboratory and, more recently, in rather large prototype pipe flow systems [1]*. In the majority of these studies, homogeneous polymer flows were utilized, either by using a pre-mixed solution of the desired concentration or by injection of a concentrated solution at the proper rate to provide a given homogeneous solution after complete mixing had taken place.

For many practical applications it is necessary to inject the polymer additive into an external boundary layer. In these cases, as the boundary layer grows downstream of the injection point the polymer concentration decreases due to dilution. Its effective concentration may also be decreased by degradation following substantial exposure to high shear rates. Several experimental investigations on a small scale have been carried out to determine the characteristics of such a flow [2,3,4,5]. In most of these cases, no information relative to the polymer concentration profiles in the boundary layer was obtained. It therefore seemed appropriate that larger scale studies be initiated in which such concentration profiles would be measured and the changes in the boundary layer characteristics could be determined. Such studies were recently carried out at the St. Anthony Falls Hydraulic Laboratory in an open channel of 9 ft width, utilizing flows with a developing boundary layer up to about one foot in thickness. Several parallel investigations were also conducted in a gravity flow pipe facility. Some of the preliminary results have been presented in earlier reports of limited distribution [6,7], and the present report supplements and supercedes these earlier reports. Results of a particular phase of the investigation have also been presented at a recent meeting [8].

---

*Numbers in brackets refer to references listed on pages 35-36.

II. EXPERIMENTAL FACILITY AND INSTRUMENTATION

A. Main Test Channel

A sketch of the salient features of the Laboratory main channel as modified for use in the experimental program is shown in Fig. 1. Before discussing the final configuration in detail it may be well to first consider the general features of the facility and the reasons for making the modifications.

Water is drawn into the channel by gravity flow from the upper pool of the Mississippi River at St. Anthony Falls and first passes through a mechanical screen of 3/8 in. mesh to remove coarse debris. The pressurized flow then passes beneath a variable-opening underflow control gate and into a vertical drop shaft. From the vertical shaft the flow turns 90° into a rectangular horizontal tunnel of 9 ft width and 6 ft 4 in. depth. The exit of this tunnel, which is 9 ft wide and 3.75 ft high, is fitted with a multiple-controlled orifice closure plate which serves to dissipate the excess gravity head of the flow as it enters the main channel.

The channel itself is largely of poured concrete construction with smooth but slightly wavy wall and floor surfaces. The width is uniformly 9 ft, the depth is about 6 ft, and the clear length is 253 ft. The channel floor has a drainage slope totalling about 6 inches in its length.

At a point 175 ft downstream of the control orifices the concrete construction gives way to a 20 ft length of steel-framed construction which supports steel-faced surface panels on one wall and on the floor. The other wall is surfaced with steel-framed glass panels for observation purposes. The entire structure of the steel section is bolt-connected to permit removal, modification, and reassembly of the surface panels.

Downstream of the 20 ft observation section the channel reverts to concrete construction for the remaining 58 ft of length. At the end of this reach is the downstream control gate by which the tailwater depth can be adjusted. The flow beyond this gate proceeds to a volumetric discharge measuring tank and then is wasted in the lower pool of the river.

The depth of flow entering the upper end of the test channel may be arbitrarily varied from zero to about 5.5 ft by suitable settings of the various gates and control devices. The turbulence level in the vicinity of

the upstream multiple orifice closure is quite high whenever larger discharges are employed. Although the turbulence is not significant to many flow studies, it was considered excessive for the current study involving diffusion processes. For this reason the decision was made to abandon the use of the upper end of the channel as the locale of the boundary layer origin and to install a new contraction mechanism in the channel further downstream. The downstream test location provided a considerable length for damping the turbulence generated by the multiple orifice energy dissipator at the upstream end of the channel.

The addition of a downstream contraction had three major benefits: first, it originated an essentially new floor boundary layer just downstream of the contraction; second, it accelerated the water to higher and more useful velocity levels; and third, it provided an essentially uniform velocity field at the origin of the new boundary layer. The redevelopment of the boundary layer depends on the ratio of the upstream and downstream depths of the contraction. The new kinetic energy values for various streamlines constituting the downstream velocity profile are derived from the sum of the pressure energy (which is converted to kinetic energy in the contraction) plus the kinetic energy existent upstream on the streamline. For relatively large depth ratios nearly all the downstream kinetic energy is derived from the pressure head differential on a given streamline. As the pressure differential is essentially constant for all streamlines, the downstream velocity will be nearly constant for all streamlines in the section. This newly formed profile at the contraction exit can therefore be considered the origin of the developing two-dimensional test boundary layer which grows downstream of this point.

An additional honeycomb was placed in the channel 130 ft downstream of the multiple-orifice to further reduce large-scale turbulence. This honeycomb had 6 in. by 6 in. openings, 36 in. long, and a thin honeycomb made up of layers of corrugated steel roofing with much smaller openings was fastened to the upstream face of the honeycomb. Observations of the flow patterns indicated that the benefits achieved by the honeycomb were marginal, and it was later removed without any apparent loss in flow quality.

The orifice bulkhead, shown as "f" in Fig. 1, was constructed of plywood sheeting supported by steel framing with the lower edge of the plywood

fitted with a brass strip to provide a sharp edge. The framing was designed to permit placement and attachment at any selected position along the channel axis. A simple bolt attachment of the bulkhead to the framing provided easy adjustment of the orifice opening and thus of the downstream depth of flow. Two openings of the sluice gate were used in the test program that resulted in about 7 in. and 13 in. depths of the test stream in the test area 16 ft downstream of the bulkhead.

The temperature of the river water varies from a summertime high of as much as 80°F to a stable winter low of 32+°F. The water is not potable, but is relatively clean. Following heavy rains or in flood flows some organic and fine mineral solids are carried in suspension, and visibility is poor. During normal or low-water summer flows mineral solids are reduced, but organic fines remain and visibility is somewhat impaired. Plant segments of finite size occasionally appear in the flow. During the cool months of the year the organic fines disappear and visibility is excellent. Extensive earlier tests with a variety of polymer additives have demonstrated compatible chemical characteristics at all seasons.

An enlarged sketch of the test reach is shown in Fig. 2. The injection slot was placed directly on the floor of the channel; details of the injection system will be discussed in the next section. For the first tests a number of impact tubes were mounted through the steel floor of the channel, as shown. These tubes were used both for velocity measurement and as fluid withdrawal sampling probes. Additional details of the tube array are given in Figs. 5, 6, and 18 of Ref. [6]. The associated manometers were located in a pit below the steel floor, so that the entire system was under positive pressure.

The array of impact tubes was used rather than traversing a single tube because of the slow time response of the flat-tipped probe, the limited duration of test runs (about three minutes at the higher injection rates), and the limited batch (10,000 lbs) of available additive. The possible spatial variations of probe values were recognized, but were compromised as being less important than adequate response time. Separate tests of the spatial variations of the array indicated that this may not be serious.

A profile of the channel bottom was taken at various distances downstream from the injection slot on lines 6 in. on each side of the channel centerline over the test reach. The datum for all measurements was established

as a point at the slot edge 6 in. to the left of the channel centerline looking downstream. The nominal floor drainage slope of the channel is one to 500, and the measured deviations from this slope are shown in Fig. 3. It is apparent that immediately after the steel floor, the slope increases for about five feet and then again reverts to a value slightly greater than one to 500.

Most test data were obtained with the floor in its original condition, i.e., trowelled concrete and painted steel. However, it was also desired to determine the existence of any adverse effects on the polymer associated with typical ship anti-fouling paints. Therefore a considerable portion of the floor of the main test channel, including the test reach, was first sand-blasted and then painted with the materials provided by the sponsor.

The steel plate area was painted with one coat wash primer Formula F-117, Mil-P-15328, FSN KZ8030-165-8577; four coats of vinyl red lead, Formula F-119, Mil-P-15929, FSN KZ8010-722-7119; and two coats of anti-fouling red, Formula F-121, Mil-P-15931, 9Q8010-682-6437. Concrete areas were painted in the same manner except that the application of the vinyl red lead was omitted.

B. Polymer Mixing and Pumping System

Concentrated solutions of Polyox WSR 301 (Union Carbide) were mixed in a calibrated supply reservoir consisting of a portable swimming pool 10 ft in diameter and 2.5 ft deep. Ten thousand pounds of solution were prepared for each run. Stock solutions were prepared by adding weighed quantities of dry polymer to a disperser installed in a water supply line as shown in Fig. 4. The disperser operates on an aspiration principle and insured that the polymer particles were dispersed and wetted as individual particles which could be readily dissolved. A propeller stirrer was used to provide a gentle agitation of the solution during the initial mixing process. The stirrer was then shut off and the solution was left for about 18 hours before being used. At this time it was found that in general, complete solution had taken place with little evidence of any gelatinous globs being present, the solution being optically clear. The mixture was again gently stirred manually with a wooden paddle shortly before use to insure

a uniform solution throughout the tank. Most tests were conducted with stock solutions of 1000 and 2000 ppm, although other concentrations were used in limited tests.

Head losses in the injection system required that a pump be utilized to provide the desired discharge. A centrifugal pump was installed in the supply line as shown in Fig. 4. The flow from the pump passed through a calibrated elbow meter and a control valve into a 6 in. diameter plenum chamber and finally through six 1.5 in. diameter manifold pipes leading to the injection slot chamber. To determine polymer degradation effects, samples were routinely collected from the tank and the exit of the injection slot during test runs and were subsequently analyzed in a blowdown rheometer.

C. Injection Slot

Details of the injection slot are shown in Fig. 5. As it was originally intended that both the orifice bulkhead and the injection slot be moved upstream at some time during the test program, the injection slot was constructed as a unit that could be attached directly to the channel floor. The height of the injection system was about one-half inch above the floor, and a 36 in. long ramp of trowelled leveling compound was provided at the upstream end of the structure to provide a smooth flow transition. The top cover of the chamber was constructed of 1/8 in. steel plate, and the steel floor of the test section was used for the lower cover. Spacer rods located at 12 in. intervals in the transverse direction maintained an essentially constant slot thickness.

The stock solution from the pumping system entered the injection chamber through the manifold pipes previously mentioned. A honeycomb about 3.5 inches in length was installed downstream of the manifold pipes as a head loss device to improve the flow distribution and to act as a flow straightener.

After installation of the slot top cover the slot opening was measured about every half foot across the slot length. The average of these measurements was 0.20 in. It was also of interest to determine the uniformity of velocity over the length of the slot. A small Pitot tube was placed at the midpoint of the slot opening, and velocity measurements were made every 6 in. for a given discharge. These measurements were made with the slot discharging as a submerged jet in a static pool, that is with no water flowing over the slot. The results are shown in Fig. 6 for the 3/16 in. nominal slot height.

For some tests later in the program the slot was partially blocked near the sides, so that the effective slot width was reduced from 9 ft to 5 ft.

D. Three-Dimensional Characteristics of the Test Flow

The main test channel of the Laboratory was originally selected for the large-scale study of a polymer-treated boundary layer because the nine foot width in company with depths of about one foot was considered to provide an essentially two-dimensional flow. It was initially appreciated that the orifice-contraction component of the system would produce substantial corner vortices at the corner edges of the flow stream (see Fig. 7 of [6]), but these were presumed to remain as minor edge effects until far downstream. Even after the initial tests with the flow system, superficial evidences indicated (see Fig. 7 [6]) that the central portion of the flow stream was essentially two-dimensional in character. This belief persisted until tests were undertaken involving the addition of Rhodamine dye to the injected polymer for purposes of diffusion evaluation. This rather intense dye not only served for this evaluation, but also proved to be a simple visual tracer of the structure of the injected flow as it was discharged from the two-dimensional injection slot which spanned the boundary of the test stream. The surprising feature of the dyed injection was that it did not persist as an integral two-dimensional wall jet, but almost immediately following injection (less than one foot downstream) gave visual evidence of forming into a row of axial streaks of dyed flow alternating with undyed water. The spacing of these streaks ranged from about 6 inches to 12 inches in a constantly wavering and varying pattern. It was first presumed that these streaks were vortices originating in some non-uniformity of the injected jet, but the Pitot probings of the injected stream failed to establish any significant abnormalities. Additional observations of these streaks with the progressive testing in the channel led to an increasing conviction that the streaks were not the result of the presence of the polymer or of the injection into the boundary, but were in fact an inherent feature of the channel flow. Attempts were then made to improve the upstream flow by eliminating any spaced sources of abnormalities, and to this end the honeycomb flow-straightener which had been located 45 ft upstream of the contraction (see Figs. 1 and 3 of [6]) was removed from the flow. The removal failed to have any influence on the dye streaking.

In parallel with these physical observations and alterations the literature was probed for possible related material. This search disclosed the following significant findings:

1. Somewhat analogous vortical streaking has been observed and reported for other ostensibly two-dimensional or nearly two-dimensional flows as follows:
   a. Small-scale curvilinear boundary layer flows
   b. Large-scale wind tunnel turbulent boundary layer flows
   c. Cloud streaking in the shear zones of atmospheric stratifications
   d. Bed-load transport of sand and snow across highways
   e. Bed-load transport of sediment in artificial channels.
2. While visual tracers have supported observations of these phenomena in nature for a long time, cognizance of their existence in research flow systems appears relatively rare because of the normal absence of suitable tracer materials and adequate perspective of observation.
3. A few recent studies have attempted to make instrumented probings and correlations of these secondary flows, but their random superposition in an already turbulent and usually unsteady flow has posed severe measuring problems.

In light of the foregoing physical observations and allied findings in the literature the following assumptions are tentatively suggested for consideration in current and future studies of injected polymer boundary layers in either laboratory or full-scale field trials:

1. Spaced vortical secondary flows are in all probability an inherent part of the momentum exchange mechanism of large boundary layers or shear zones.
2. Spaced vortical flows have been observed in straight open channel flows and may be presumed to exist in external body flows, particularly for bodies of concave external curvature.
3. Point-source instrumentation for the evaluation of shear, boundary layer structure, or polymer diffusion must recognize the existence of the wandering secondary flow as a significant large-scale low-frequency time transient.

4. Pending a better understanding of these secondary flows it is suggested that all point-source instrumentation employ long-time sampling.

5. It is probable that the most realistic shear flow measurements can be obtained only with a sensor of large area extent.

Later in the experimental program a velocity survey was made across the width of the channel at a location 16 ft downstream of the injection slot. Pitot tubes were laterally spaced at approximately 0.75 ft intervals and set at the same vertical distance from the floor boundary. These studies were undertaken to further determine the character of the flow at greater lateral distances from the channel centerline than were previously utilized. Some of the results are shown in Fig. 7 at a distance of 0.1 ft from the boundary. The velocity distribution for about 2.5 ft on each side of the centerline was fairly uniform. As the channel sidewall was approached the velocity first decreased, then increased significantly in the region of the corner vortex. The data taken with polymer injection follow the same general trends. This indicates that for about a 5 ft span of the channel the flow is essentially two-dimensional at this downstream location.

E. Impact and Sampler Tubes

For measurements made at a station 16 ft from the injection slot it was most convenient to insert the impact tubes through the steel floor, as shown in Fig. 2. At larger distances from the slot the floor of the channel was concrete, and a different method of probe mounting was required. A large wooden box was constructed that could be placed directly in the channel. The box was supported by steel legs of small diameter, with the box itself being above the test stream. The structure could be readily moved to any longitudinal position in the channel. With this system the impact tubes passed downward through the free surface, and it was necessary to resort to larger diameter stems to provide structural rigidity. In all cases the same tubes were used for both velocity measurements and withdrawal of samples of fluid from the boundary layer.

The tubes mounted through the floor were made of 0.252 in. O.D. stainless steel tubing. The stagnation end of the probe was crushed over a 16 gage metal plug for a 5/8 in. length and was then ground to provide a

1/32 in. wall thickness top and bottom. The stem of the tube was supported by a brass sleeve fitted in the steel floor, and suitable fittings were provided to permit positioning of the tube from below the floor. A tee fitting was attached to the stem beneath the floor with one line leading to the manometer system for velocity measurements and one line leading to the collection system used for sample withdrawal.

Static pressure was measured with a 3/16 in. diameter piezometer tap drilled in a brass plug installed in the steel floor. After installation the plug was hand-finished flush with the floor. The selection of the tap size was quite arbitrary. It was felt that any hole from about 1/16 in. to 3/16 in. in diameter would differ little in dynamic pressure errors. After consideration of the silty river water existing at the time of the tests and the need for a small response time on the manometers, use of a hole smaller than 3/16 inches in diameter was not deemed practical.

The difference between stagnation and static pressure was measured on a multi-tube manometer. Meriam No. 3 (specific gravity 2.95) was used as the gage fluid for measurements taken at the steel floor section. A purging system utilizing city water pressure was installed to clean the lines of air and also to remove any organic material that may have collected on the tips of the impact probes. In some cases it was necessary to use compressed air to remove fouling material. The entire system was normally continually purged with city water until actual measurements were obtained. Attempts to use smaller impact tubes were abandoned due to continued plugging by organic material which could not be removed by the purging system.

The stems of the tubes used at other than the 16 ft station were constructed of 0.50 in. O.D. brass tubing with a wall thickness of 0.125 in. for structural rigidity. Support of the stem was provided in the previously mentioned wooden box above the test stream. The impact probe itself was a 0.252 in. O.D. tube attached to the larger supporting stem. Again the end was bent and flattened so that measurements closer to the wall could be obtained. Water depth was measured with a point gage. Repeated measurements of the water depth were made during a given test run and averaged.

The impact tubes were connected to transparent manometer tubes and the velocity was determined from the height of the water in the tubes above the

water surface. Organic material collecting on the probe tips was removed before each test by blowing compressed air through each tube.

It should also be mentioned that both types of impact tubes were calibrated in a laboratory calibration facility over the range of velocities encountered in the tests. No corrections were found to be necessary. The tubes were calibrated in water only; no calibrations were made in dilute polymer solutions. Based on previous work with impact tubes in polymer flows [9] it was felt that corrections would not be significant for these relatively large tubes and the generally low concentrations of polymer in the boundary layer.

When the impact tubes were used for withdrawal of samples a connected plastic diversion hose was valve by-passed to feed into a collection bottle. Flow was motivated by the inherent stagnation pressure of the flow. Detailed tests of withdrawal at various valve-controlled rates indicated that the sample concentration was not sensitive to the withdrawal rate. To assure a relative insensitivity to temporal variations of the homogeneity of the flow, as discussed in Section D, samples were withdrawn for continuous periods of not less than two minutes.

F. Sample Analysis

Three different methods were investigated and evaluated for determination of the polymer concentration in a particular withdrawal sample. A fourth method previously used for smaller-scale studies at this laboratory was not considered practical for the larger-scale tests. This method employed the addition of a food dye to the concentrated polymer solution and analysis of the sample for dye content with a colorimeter. As the limited sensitivity of the colorimeter required excessively large quantities of dye to be added to the stock solution, this method was abandoned. The three methods that were considered are discussed below.

1. Polarography

Polarography is a well-established tool of chemical analysis. Basically, polarography is a study of the relationship between current and potential in an electrolytic cell consisting of a dropping mercury electrode placed in an

electrolyte. The dropping mercury electrode is a vertical capillary tube attached to a mercury reservoir. Mercury passes through the capillary and exits in discrete drops, thus providing a continuously renewed surface. The relationship between the current and the potential for the cell can be related to electro-chemical processes taking place at the dropping mercury electrode. Progressive increasing of the applied potential results in an increase in the current until a plateau is reached which is proportional to the concentration of metallic ions in solution. The plot of current against applied potential is referred to as a polarogram. With aqueous solutions the presence of dissolved oxygen results in a sharp maximum in the polarogram. For most analyses this maximum is not desirable and is usually suppressed by the addition of surface-acting agents to the electrolyte. Suppression of the maximum is proportional to the concentration of the surface-active agent. Polyox WSR-301 is a surface-active agent which responds as a suppressant. The method was first reported in detail by Goren, et al. [10], and was later used in evaluating polymer concentrations in laboratory pipe flow tests [11].

A simple polarograph was constructed at the laboratory for evaluation and possible use in the test program. It was possible to obtain a calibration of the suppression of the oxygen maximum as a function of Polyox concentration. It must be recognized, however, that the calibration was valid only for a given solvent, drop rate, and solution temperature. Check tests have indicated that the concentration of premixed solutions could be determined to within 5 ppm. With carefully controlled conditions the polarograph appears to be a useful tool in determining Polyox concentration in a given sample.

However, for the large-scale tests of the current program river water was used as the solvent. The level of dissolved oxygen was extremely variable, and in some instances an oxygen maximum could not be obtained with river water alone. Water temperature also varied widely. As a result of such difficulties the method was not given further consideration, and alternative methods were sought.

2. Turbidimetric Method

Through communication with personnel at Union Carbide Corporation a direct method of determining Polyox concentration was made available and is

fully described in Ref. [12]. The method is based on the reaction of Polyox and poly (acrylic acid) to produce a precipitate. This molecular association product was found to form only with poly (ethylene oxide) of molecular weights greater than 100,000. The turbidity produced by the precipitate is then determined with a spectrophotometer, or equivalent, and is proportional to the concentration of Polyox in the sample.

This method was investigated at the laboratory according to the detailed procedure given in Ref. [12]. A quantity of poly (acrylic acid) and reagent was prepared. To obtain a calibration curve, samples with concentrations of 10, 20, 30, 40, and 50 ppm of Polyox were mixed with river water. A spectrophotometer for turbidity analysis was not available. However, it was found that with the use of a filter with an approximate spectral range of 400 to 465 millimicrons, a Klett-Sommerson photoelectric colorimeter could satisfactorily be used for the turbidity measurements.

The following procedure was adopted:

a. Equal quantities (5 ml) of the poly (acrylic acid) reagent and the test samples were prepared in a test tube with a pipette. After gently shaking, the mixtures were permitted to stand for one hour.

b. Colorimeter readings were taken with samples of river water and reagent for zero reference.

c. Colorimeter readings were taken with samples containing Polyox and a plot was made of colorimeter reading vs. concentration. The calibration was found to be linear for concentrations between 5 and 30 ppm. In the analysis of samples with unknown concentrations expected to be out of this range the samples were further diluted to produce colorimeter readings corresponding to the linear portion of the calibration curve.

The turbidimetric method appeared to provide consistent measurements as determined by check tests of the calibration. Extreme care was required in the experimental technique to avoid contamination of either the sample itself or the containers in which the samples were prepared or collected. For example, it was found that wiping the test tubes with a commercial clean white cloth resulted in considerable scatter of the data (presumably due to chemicals used in manufacturing the cloth). This scatter could be minimized by wiping the test tubes with a paper towel dampened with distilled water. Also,

the preparation of the poly (acrylic acid) reagent was time-consuming, although not difficult.

3. Fluorimetric Method

In this method small quantities of a compatible dye were added to the concentrated stock solution of Polyox. Samples collected from various points in the boundary layer were then analyzed for dye content. It was assumed that the diffusion of the dye and the Polyox was the same and that thus the polymer concentration could be obtained from a calibration curve.

The colorimeter could have been used for analyzing the samples. However, the sensitivity of the instrument required that relatively large quantities of dye be added to the stock solution. To circumvent this problem a Turner Model 111 Fluorimeter was used for sample analysis. Later in the program an American Instrument Co. Model No. 4-7390 Fluoro-Microphotometer replaced the Turner instrument. These particular instruments have been widely used in many studies related to the detection of very minute quantities of dye tracers. It was necessary to use a fluorescent dye tracer, one which was not normally present in the river water. Rhomadine B was selected for this purpose. Rhomadine B was found to be compatible with Polyox in that it was stable and did not influence the drag-reducing properties of the polymer, as was determined with a capillary tube blowdown rheometer.

A calibration curve was obtained by using samples of known dye concentrations mixed with river water. Samples of river water only were first analyzed, and this slight threshold reading was subtracted from the readings taken with the dye samples. It was necessary to base the calibration on the difference between the two readings, since the quality of the river water used as the solvent varied over a rather wide range. The calibration indicated that a linear relationship existed for dye concentrations of less than one ppm. For cases where the concentration was expected to be greater than one ppm, the sample was diluted a known amount. Check tests on the calibration indicated that the instrument was stable over long periods of time. To account for calibration changes due to temperature variations, the samples and calibration standards were analyzed at the same temperature.

In general it was found that use of the fluorimeter permitted rapid determination of dye content in a sample. However, it must be recognized that extreme care was required to prevent contamination of a sample. Certain types of plastics are known to contain plasticizers or materials which will fluoresce. Since extremely small quantities of fluorescent material were being analyzed, even a fingerprint on the cuvette containing the sample resulted in large errors. It was found necessary to wipe each cuvette with a moistened paper towel before inserting in the instrument. Wiping with a clean white rag caused a wide variation in readings. Detergents could not be used for cleaning the cuvettes, as detergents are known to fluoresce and thus introduce errors.

G. Blowdown Rheometer

A capillary tube rheometer was used to monitor the test solutions. The rheometer is similar in principle to the Ostwald rheometer with the exception that the driving pressure is variable through use of the laboratory compressed air system. The length of the capillary tube was 1000 diameters, and thus any corrections due to entrance effects were assumed negligible. Degradation of the polymer may have occurred over the extended length. However, as the rheometer was used only to determine relative drag reduction effects, this did not appear to be important. Fluid issuing from the tube was collected over a given time interval and weighed to determine the discharge. Collection times were sufficiently long to reduce errors in timing. Tests were first made with distilled, tap, and river water as reference values. No differences were found in the pressure drop-discharge relationships for these fluids. Results were also obtained in the turbulent flow regime with dilute polymer solutions of various concentrations expected to be encountered in the test program. As dye was to be added to the concentrated solutions used in the main channel tests, samples containing small amounts of Rhodamine B dye were also prepared. It was found that Rhodamine B had no effect on the friction-reducing properties of dilute Polyox solutions.

The above-mentioned rheometer was developed in conjunction with earlier investigations of polymer flows, and due to its availability it was used in the current program. A rheometer of this type was found not

to be convenient to use for rapid monitoring of test solutions. For example, relatively large quantities of fluid were required to conduct a complete test. The solution was discarded after one pass through the system to eliminate any additional shear degradation effects. Furthermore, it was not possible to run a test at a predetermined shear rate. If comparisons were to be made at a given shear rate, a range of tests was required to establish friction reduction at that value.

H. Gravity Flow Pipe Facility

Attempts to determine boundary shear values in the test set-up by use of velocity profiles from the impact tubes established that a high degree of confidence in the values could not be had because workable impact tubes could not approach sufficiently close to the boundary.

In an effort to obtain an independent method of measuring local boundary shear stress in the main channel boundary layer studies, a flush-mounted hot-film sensor was also used. This sensor was calibrated in a 4 in. steel pipe. The pipe diameter was selected to provide boundary shear values comparable to those encountered in the main channel studies when the pipe was being operated with a limited gravity head available for the pipe flow system. It was also essential that the pipe diameter be large relative to the 0.125 in. diameter of the flat face of the probe to reduce the effects of surface curvature. A schematic layout of the gravity flow pipe facility is shown in Fig. 8. Fifty feet of pipe were laid horizontally, with the test section located 114 diameters downstream of the beginning of the straight reach. Water was drawn directly from the Mississippi River and was discharged to waste under a 50 ft head. Discharge was controlled using the gate valves and was measured with a calibrated metering elbow. A flow straightener consisting of 3/4 in. tubes about 1.5 ft long was placed at the pipe entrance to reduce the effects of the upstream elbow. Four 1/8 in. diameter piezometer taps were carefully drilled and deburred at each of the locations shown. Pressure drops used in the calculation of wall shear stress were measured over each of the distances shown as well as over the entire test reach of 10 ft. Preliminary tests indicated that the pressure gradient was constant and the flow was fully developed at the test section.

Aqueous solutions of poly (ethylene oxide) WSR-301 with concentrations of 250 and 500 ppm by weight were mixed in a large storage tank located at a higher level in the laboratory. Gentle agitation was used in mixing. A low head pump was used to transfer the polymer from the tank to the pipe, and the polymer was injected at the low pressure side of the upstream elbow, as shown in Fig. 8. The injection rate was determined by measurement of the drop in fluid level in the calibrated storage tank for a given period of time. The concentration of the homogeneous polymer solution in the test section was calculated from the injected and pipe discharges.

The polymer solutions were analyzed for drag-reducing properties with a capillary tube blowdown rheometer. A sample withdrawn from the pipe at the test section was checked against a sample collected from the storage tank and diluted to the calculated concentration. The results agreed satisfactorily, indicating that complete mixing had taken place and that degradation effects were minor.

A Thermo-Systems, Inc., Model No. 1237W flush-mounted sensor was installed at the location shown in Fig. 8. The sensor was attached to a traversing mechanism to permit movement along a radius of the pipe as well as rotation about this radius as axis. Radial position was measured with an Ames dial micrometer reading to within 0.001 in., and the rotation was measured with a protractor accurate to one degree. The cold resistance of the sensor was measured before and after each test run and was found to be very stable. An overheat ratio of 10 per cent was used in all tests.

The output of the anemometer was fed into various electronic components for further processing. Average bridge voltage was measured with a Weston digital voltmeter modified to give a 10-second integrating time. The rms of the fluctuating signal was measured with a Disa Random Signal Indicator and Correlator, Type 55A06, which was also used for direct measurement of the microscale. Frequency analysis was carried out with a Hewlett-Packard 300H harmonic wave analyzer having an 11 Hz effective bandwidth. The signal from the anemometer was also fed into a high-gain amplifier, whose output in turn was connected to a Hewlett-Packard electronic counter. The counter was capable of sensing the number of positive crossings of a zero reference level of the amplified bridge voltage fluctuations per unit time.

Velocity profiles were also measured for various homogeneous polymer concentrations and Reynolds numbers. A flattened impact tube with an opening of 0.015 in. was used for these measurements. It was noted that for a polymer concentration of 20 ppm the measured velocities were less than the true velocities. This discrepancy became apparent in the comparison of the measured discharge and the discharge obtained from integration of the velocity profiles. The integrated values were about 20 per cent less than the measured values. For the lower concentrations no significant discrepancies were noted. Similar behavior for impact tubes towed through homogeneous Polyox solutions have been reported [9].

III. TEST RESULTS AND DISCUSSION

A. Water Velocity Profiles in the Large Channel

The first tests in the main channel were conducted with water alone to check out the instrumentation and determine the characteristics of the boundary layer. Typical profiles are shown in Fig. 9 taken at x-distances of 16, 28, and 40 ft downstream of the injection slot and with corresponding x_1-distances of 21, 33, and 45 ft, respectively (see Fig. 2). The displacement thickness δ_* has been used to render the normal distance from the boundary floor dimensionless. The data indicate that essentially similar profiles exist at these three measuring stations. Measurements were also made of the transverse velocity distribution across the impact tube array, and variations of the mean velocity were found to be minor, as previously reported [6]. Figure 7 shows that the velocity distribution at the 16-ft station was fairly uniform across a 5-ft section through the center of the channel. To further establish that the grouping of impact tubes was not creating spurious effects a single tube was traversed vertically through the boundary layer. Experimental data at the 16-ft station are plotted on semi-logarithmic paper in Fig. 10, and the results for the single and arrayed tubes agree satisfactorily. Similar behavior was noted at the other measuring stations. The distance from the boundary, y, was taken as the distance from the center of the tube to the boundary with no corrections being applied.

It was of interest in the tests to determine both the total and the local drag coefficients from the measured velocity profiles. By integration

of the velocity profiles, the momentum thickness θ was obtained. Assuming that the pressure gradient was zero, the total drag coefficient was $2\theta/x'$ where x' is the distance from the origin of the boundary layer. An approximation of the virtual origin of the boundary layer was established for this purpose by plotting the momentum thickness as a function of the distance from the slot, and these data were then extrapolated to the point where the momentum thickness was zero. It was found that the virtual origin was about 4.5 ft upstream of the slot, and this length was added to the measured distance from the slot. The resulting value was used as the reference length in the Reynolds number and in other calculations involving the position of the origin of the boundary layer. It was assumed that the origin was not affected by polymer injection, and thus, as will be noted later, the origin was not a factor in determination of drag reduction.

The total drag coefficient determined in the above manner for water flow is shown in Fig. 11(a) for several Reynolds numbers. As the velocity did not change greatly in the downstream direction, the change in Reynolds number was achieved through variation in length and kinematic viscosity. The seasonal variation in temperature results in nearly a twofold change in kinematic viscosity. Typical trends associated with the change in viscosity are shown by the two sets of data taken at the 16-ft station. It should also be noted that the crossed symbols represent data taken after the channel floor had been painted as described earlier. These points fall essentially in the same groupings as for the unpainted floor, indicating little effect of the paint on the boundary layer characteristics for water flow.

Local shear stress evaluations were made from the measured velocity profiles. The data were plotted on semi-logarithmic paper as shown in Fig. 10, and the shear velocity u_* was inferred from the profile by drawing a straight line through the data near the boundary. Assuming that

$$u = \frac{2.3\, u_*}{k} \log y + C \qquad (1)$$

where $u_* = \sqrt{\frac{\tau_o}{\rho}}$ and C = constant, the slope of the line determined u_* for a given value of the Karman constant k, taken to be 0.4 in all cases. The local drag coefficient as calculated from u_* is plotted in Fig. 11(b) as a function of Reynolds number. It was also possible to plot

dimensionless profiles in terms of the law of the wall and the velocity defect law. These plots will be discussed in the next section.

It should be mentioned that the above method of determining the local shear stress is subject to some error, as the shear velocity is very sensitive to the slope of a line drawn through a rather limited number of velocity points. Difficulties associated with foreign material in the river water discouraged the use of a greater number of tubes in the array or of smaller tubes to permit evaluations closer to the boundary.

If sufficient data points of the velocity profile are available, the method of determining local shear stress is probably more accurate than the method of determining total shear stress by momentum deficiency. The two methods do not seem to agree at the 16-ft station, where the local shear stress coefficient is nearly smooth while the total is much rougher. This might be due to an effect of the injection slot on the momentum equation. It might also be due to greater relative roughness near the origin of the boundary layer where the boundary layer is thin, but this is negated by the increased roughness for greater x in Fig. 11(b).

B. Typical Velocity and Concentration Profiles with Polymer Injection

Velocity and concentration profiles were plotted for nearly every test run. Since many of these profiles have been presented earlier in [7], they will not be presented here. A typical set of data is shown in Fig. 12 for a concentration of the injected polymer solution, c_i, of 1000 ppm. It can be readily seen that polymer injection resulted in a much fuller velocity profile than did water injection, implying corresponding decreases in the displacement thickness δ_* and the momentum thickness θ. For any given test the shear velocity was reduced by the polymer as determined by semi-logarithmic plots of the velocity profiles.

Data could not be obtained sufficiently close to the boundary to detect changes in the inner velocity gradient. However, a crossing of the velocity profiles near the wall has been observed for high injection rates and solution concentrations. It is possible that this may be associated with relatively high concentrations of polymer at the wall resulting in errors in velocity measurement.

As noted earlier, polymer concentration was determined by analysis of a given sample for dye content and also by measurement of the turbidity due to precipitates formed by addition of analytical chemicals. A comparison of the concentrations measured by these two methods is shown in Fig. 12. As the agreement was satisfactory in this test as well as in others not shown here, the bulk of the concentration samples collected during the test program were analyzed only for dye content on the assumption that the dye and polymer diffused similarly.

The maximum concentration was found at or near the wall. Concentration decreased with increasing distance from the wall and was essentially zero at the outer edges of the boundary layer. Further discussion of the concentration profiles is deferred to Section III D.

For two-dimensional flow and constant fluid density the continuity relationship for the injected fluid is, to a good approximation,

$$q_i c_i = \int_0^\infty uc \, dy \qquad (2)$$

where q_i is the discharge per unit width.

This relationship was evaluated for all measured velocity and concentration profiles and compared with the measured input. It was found that in most cases the integrated value was larger than $q_i c_i$ by magnitudes larger than could be attributed to errors in the measurements. This discrepancy was also noted in tests with injection of dyed water, and was therefore not associated with any peculiar behavior of the polymer additive. Observations of the dyed solution injected from the slot have indicated a lateral contraction of the dye stream immediately downstream of the slot. The vortices in the corners of the channel, as previously described under D of Section II, are believed to be partially responsible for the observed contraction. The observed streaking or non-uniformity of the injected fluid may also have contributed to some error.

In further evaluation of the two-dimensionality of the flow, transverse velocity profiles had indicated (Fig. 7) that the velocity was essentially constant across a 5-ft width in the center of the channel. The

injection slot was partially blocked to provide a 5-ft central width instead of the full 9-ft width of the channel. Observation of the issuing dye stream revealed little or no lateral contraction or expansion of the dye stream at the 16-ft station. After analysis of the data collected with this modification, much better agreement was found with the continuity relationship. Differences between the integrated and injected values were reduced in many cases to less than 10 per cent as opposed to an average of about 30 per cent for tests conducted with the 9-ft slot width.

C. Dimensionless Velocity Profiles - Main Channel

Using the shear velocity inferred from semi-logarithmic plots of the velocity profile, the profiles were plotted in non-dimensional form according to the law of the wall and the velocity defect law. In the region near the wall,

$$\frac{u}{u_*} = \frac{2.3}{k} \log \frac{yu_*}{\nu} + B + \Delta B \qquad (3)$$

where k is the mixing length constant (assumed to be 0.4), B is a constant dependent on the boundary roughness ($B = 5.5$ for a smooth surface), and ΔB is a parameter associated with the drag-reducing properties of the polymer.

Some typical data are plotted in dimensionless form in Fig. 13 to indicate the effects of polymer injection on the velocity profile. If attention is first confined to the profiles for water flow only, as shown by the open symbols, the downward shift of the profile indicates that apparently the effective roughness of the boundary is larger at the 40-ft station, on the concrete surface, than at the 16-ft station, on the steel surface. Following the injection of polymer the profiles are shifted vertically upward from the corresponding profile for water flow. This shift is the ΔB in the above equation, and the measured and averaged ΔB values from the plot are tabulated in Fig. 13. The trends shown support the concept of the "negative roughness" analogy in that the addition of polymer to the flow results in a positive ΔB, whereas the influence of boundary roughness results in a negative increment B when referred to the smooth boundary case.

If the velocity profiles are plotted according to the velocity defect law, the experimental data for both smooth and rough surfaces can be expected to fall on one line, as it is known that the velocity defect is essentially independent of roughness. The velocity defect is generally plotted as a function of the ratio of the distance from the boundary to the boundary layer thickness. Since the limited number of data points available for the velocity profile made it somewhat difficult to accurately determine the boundary layer thickness, the parameter $yu_*/U\delta_*$ was used for the abscissa. Typical results are plotted in Fig. 14, again with the open symbols used for water flow and the filled symbols used for flows with polymer injection. The polymer data tend to conform to a common line with the water data. A comparison with the results of Clauser [13] is also shown for reference purposes.

D. Dimensionless Concentration Profiles

Variation of polymer concentration throughout the boundary layer at the 40-ft station for various rates of injection of a 2000 ppm solution are shown in Fig. 15. As the injection rate was increased, the concentration at the boundary, c_o, also increased. A similar effect can be achieved by increasing the concentration of the injected solution. The quantity of polymer injected into the boundary layer is equal to $q_i c_i$, and the corresponding variation in c_o with $q_i c_i$ is shown in Fig. 16. Crossed symbols are used for data obtained after the floor had been painted. At 16 ft from the injection slot it can be seen that relatively high wall concentrations are attained for the larger quantities of injected polymer. At further distances from the slot c_o decreases as a result of dilution in the boundary layer.

For many of the tests it was found that the concentration profiles could be correlated by plotting y/λ versus c/c_o where λ is an arbitrarily chosen parameter equal to the value of y where $c = 0.5\, c_o$, as shown in Fig. 15. This relationship has been previously developed by Poreh and Cermak [14], and was based on diffusion studies of ammonia gas injected from a line source into a developing boundary layer in a wind tunnel. Their results indicated that a final zone of mixing had been reached when the plume due to the injected gas and the boundary layer

developed thereafter in the same manner, and λ/δ attained a constant value of 0.64. The ratio of the distance from the source to the average boundary layer thickness was about 60 at this point. It has been further shown by Morkovin [15] that the following empirical relationship fits the experimental data of [14] quite well in this region:

$$\frac{c}{c_o} = \exp\left[-0.693\left(\frac{y}{\lambda}\right)^{2.15}\right] \tag{4}$$

The concentration profiles obtained in the current program have been reduced using the above ratios. Data for dyed water (no polymer additive) are plotted in Fig. 17 for various downstream distances x from the injection slot and several injection discharges. All the data were taken with the orifice bulkhead located 5 ft upstream of the injection slot except for the last data in the legend, for which the bulkhead was 29 ft upstream of the slot. The crosses on the data points indicate that the data were taken after the application of anti-fouling paint to the channel floor. It can be seen that in general the data fit Morkovin's empirical relation quite well.

Typical dimensionless concentration profiles for a water flow injected with polymer are shown in Figs. 18 and 19. All the available profiles have not been plotted. In Fig. 18 for initial injected concentrations of 500 and 1000 ppm and distances of 16 and 28 ft the data follow quite closely the empirical equation previously shown to be valid for dyed water. The profiles obtained following the injection of polymer into a thickened boundary layer are also quite similar to the other profiles.

For an initial concentration of 2000 ppm, the mixing in the boundary layer is not generally complete. With reference to Fig. 19 it can be seen that at $x = 16$ ft the concentration profile deviates from the expected profile as the injection rate is increased. For profiles measured further downstream the deviation is reduced with increasing distance from the injection slot, and final zone mixing is approached. The single test run carried out with an initial concentration of 3000 ppm further illustrates the possibility of incomplete mixing even at the 40-ft station for very concentrated solutions.

In order to predict the concentration of polymer additive throughout the boundary layer it is necessary to relate the parameters λ and

c_o to boundary layer characteristics and to the quantity of polymer injected.

Fabula and Burns [16] originally suggested the application of Eq. (4) to the present data and have developed a method of relating these concentration parameters to known quantities. They assumed that the dimensionless concentration profiles were represented by Eq. (4) and that the final mixing zone had been reached. The following equations were suggested, using the momentum thickness as the characteristic length in the boundary layer:

$$\frac{U\,\theta\,c_o}{q_i c_i} = 3.78\,(0.606\,\frac{U}{u_*} - 3.13)^{-1}\,(1 - 6.64\,\frac{u_*}{U}) \qquad (5)$$

and

$$\frac{\lambda}{\theta} = 0.15\,\frac{U}{u_*}\,(1 - 6.64\,\frac{u_*}{U})^{-1} \qquad (6)$$

A comparison of the above equations with experimental data for both dyed water and polymer flow is shown in Fig. 20. For the selected data shown in Fig. 20 the difference between $q_i c_i$ and the integrated value was less than 20 per cent. Also, the final mixing zone had been reached as indicated by the dimensionless concentration profiles and the values of λ/θ. Good agreement between Eq. (5) and the data is noted. However, the prediction of λ by Eq. (6) appears to be consistently low. This discrepancy may be associated with the measured concentrations being slightly higher than expected, thus resulting in a larger value of λ.

If data were plotted for which complete mixing had not taken place, the high concentration at the boundary would result in a much larger value of $U\theta c_o/q_i c_i$ and a much lower value of λ than predicted.

E. Drag Reduction

Drag reduction due to polymer injection into the boundary layer has been determined from the momentum thickness and the shear velocity inferred from the velocity profiles. Assuming a zero pressure gradient, the total drag reduction, ΔC_D, at a given Reynolds number was calculated from

$$\Delta C_D = \frac{C_{Dw} - C_{Dp}}{C_{Dw}} = \frac{\theta_w - \theta_p}{\theta_w} \qquad (7)$$

where the subscripts w and p refer to values for water and polymer respectively. The momentum thickness has been determined by integration of the velocity profile. Total drag reduction has been plotted as a function of polymer injected for various polymer concentrations and distances from the injection slot in Fig. 21. At the 16-ft station several interesting points should be noted. As the quantity of polymer injected is increased, the drag reduction increases until a maximum is reached, then decreases. The decrease in drag reduction was found for an injected concentration of 2000 ppm. As the injected concentration was decreased, in general the polymer seemed to be more effective. This behavior is apparently associated with the mixing of the injected polymer in the boundary layer. The dimensionless concentration profiles for the larger injection rates and polymer concentrations have indicated that final zone mixing has not taken place, resulting in rather large concentrations at the boundary. From studies of pipe flow, similar trends have been noted in that an optimum concentration exists above which the drag reduction decreases. It also should be noted that the data for the two lower injected concentrations were taken at a water temperature of about 34°F, whereas the other data were taken at temperatures varying from about 50° to 75°F. It is possible that solution temperature may also be important, as the concentrated solution appeared to have a different consistency at the lower temperatures than at the higher temperatures. Unfortunately, all samples of the polymer monitored in the blowdown rheometer for drag reduction properties were evaluated at a temperature of about 80°F, and no differences were noted under these conditions.

The crossed symbols represent data taken after the channel floor had been painted. At the higher initial concentrations the data compare well with previous data with the unpainted floor. However, at the lower concentration, 500 ppm, the drag reduction appears to be somewhat less than expected. This discrepancy is being investigated further.

At the greater distances from the injection slot the previously noted decrease in drag reduction with injected polymer was not generally found, probably because of limitations on the available injection discharge. Also, at the larger distances the polymer is diluted in the growing boundary layer, and the wall concentration becomes smaller, as previously seen in Fig. 16. One test was conducted with an initial concentration of 3000 ppm,

and the data point is shown at the 40-ft station. Drag reduction was not as large as for the lower concentrations. This discrepancy can again be related to mixing of the polymer in the boundary layer, as final zone mixing did not occur for a concentration of 3000 ppm, even at the 40-ft station.

Wu [5] has presented experimental data obtained by injection of various polymer concentrations along a flat plate on a much smaller scale. Similar trends may be noted in his data, and the recommendation was made that lower initial concentrations be used to obtain higher drag reductions. The values of $q_i c_i$ used in his work are much smaller than in the current studies, yet the drag reduction was somewhat greater. This difference may be associated with the diffusion patterns' being different in the small- and large-scale studies. Unfortunately, Wu did not measure concentration profiles in his work.

The data of Fig. 21 can also be plotted in terms of the weight of polymer injected per foot of channel width to achieve a given total drag reduction. These data are shown in Fig. 22, and a drag reduction of 35 per cent requires an injection of about 0.004 lb/sec/ft of Polyox for a boundary length of about 40 ft.

The reduction of total drag coefficient with polymer injection as a function of concentration at the boundary is shown in Fig. 23 for the three distances from the slot. It appears that the maximum drag reduction is obtained for a concentration at the boundary of about 30 ppm. This maximum is more clearly noted for the 28- and 40-ft stations, although it appears that the concentration can increase to nearly 40 ppm before a decrease in drag reduction is noted.

Local drag reduction due to injection of polymer additive as a function of concentration at the wall is shown in Fig. 24. The shear velocity was converted to a local skin coefficient, C_f, defined as

$$C_f = 2\left(\frac{u_*}{U}\right)^2 \tag{8}$$

with the drag reduction at a given Reynolds number then determined from

$$\Delta C_f = \frac{C_{fw} - C_{fp}}{C_{fw}} \tag{9}$$

It should be noted that the data for concentrated solutions of 500 ppm or less result in larger drag reductions than the higher concentrations. This trend has been noted previously in the total drag reduction plots in Fig. 21. Also, the data for the lower concentrations were taken at a lower water temperature, as mentioned before.

White [17] has proposed the following approximate expression for the local skin friction coefficient with polymer additive:

$$C_{fp} = C_{fw} \exp(-\frac{k}{7} \Delta B) \tag{10}$$

where k is the mixing length constant. Using this relationship, the local drag reduction is

$$\Delta C_f = 1 - \exp(-\frac{k}{7} \Delta B) \tag{11}$$

and thus the data of Fig. 24 also reflect the variation of ΔB with concentration at the boundary. If ΔB is calculated from Eq. (11) for the data shown in Fig. 13, the values are 5.9, 7.7, 8.2, and 4.7 as compared to the measured values of 4.4, 6.8, 8.3, and 3.0 respectively.

F. Flush-Mounted Hot-Film Sensor

Before attempting to obtain a calibration curve for the sensor as a function of boundary shear stress in the gravity flow pipe facility, considerable effort was expended to determine the influence of the location and orientation of the sensor with respect to the pipe wall. To this end the radial position of the sensor face was varied near the wall and the position of the axis of the linear heater element was rotated. The most useful signals were obtained when the heated element was placed so that the smallest dimension was parallel to the flow. For the radial position studies the entire sensor was moved systematically into the flow or into the pipe wall and the corresponding time-averaged bridge voltage and rms voltages were noted. These tests were conducted for various velocities in water flow only. It was noted that for each velocity a small range of radial positions existed for which the time-averaged bridge voltage and the rms voltage were at a minimum and essentially constant. The extent of this radial range was dependent on velocity, decreasing as the velocity increased. This small radial

range of position of the sensor included the flush position as determined visually and by touch. Therefore for all succeeding tests the sensor was located as nearly flush as possible by simple visual inspection.

The calibration curve is shown in Fig. 25 in the form of the time-averaged bridge voltage squared against the cube root of the wall shear stress. The open symbols represent data for water and the filled symbols represent data taken with polymer injection. As the concentration of Polyox was increased, the shear and bridge voltage were reduced, but not in accordance with the relationship obtained with water. At a given shear stress the bridge voltage, and thus the heat transfer, was less than that for water. This result is somewhat different than previously reported [7]. The data of [7] were taken with an earlier model of the hot-film sensor. Following eventual failure of the sensor it was replaced with a unit of much higher quality with which the present data were obtained. Thus it is felt that the data presented here are more reliable.

The number of times that the positive-going fluctuating output voltage of the anemometer crossed a given voltage reference level was also measured. These zero crossings have been plotted as a function of the square root of the wall shear stress and are shown in Fig. 26. The data for water flow are shown with open symbols and those for polymer flow with filled symbols. For the range of shear stress available in the 4-in. pipe, fairly good correlation of the data is noted. Some preliminary data on zero crossings have also been taken in a rotating drum facility at this laboratory under terms of another contract. It was possible to obtain higher speeds and shear stresses than were obtained in the 4-in. pipe. Using the same zero counting system, it is interesting to note that the data (triangles) agree well with the 4-in.-pipe data in the region of overlap and form an extension of the pipe data at the higher shear stresses. This result was encouraging, as perhaps this method could be used for measuring local wall shear stress without requiring an absolute calibration of the hot-film sensor. It should further be mentioned that different sensors, although of the same type, were used for the measurements in the two facilities. Also, constant temperature anemometers are known to be quite noisy, and this noise was partially filtered out for the data shown. More extensive studies are currently being undertaken with signals of varying levels to more firmly establish the validity of the above technique.

A typical set of data for the frequency spectra of the turbulent fluctuations obtained in the 4-in. pipe is shown in Fig. 27 for various polymer concentrations. The higher frequencies are attenuated as the polymer concentration is increased. Also, the measured rms of the fluctuating output voltage decreases slightly with increasing concentration.

A plot of the dimensionless power spectral density of the turbulence fluctuations is shown in Fig. 28 using a Strouhal number based on the pipe diameter D and the average velocity V. The power spectral density per unit band width, F(n), has been normalized with the measured mean square voltage of the fluctuating signal. The data for water (open symbols) reduce quite well, whereas the data for polymer (filled symbols) again indicate attenuation at the higher frequencies.

The integral of the second moment of the power spectra over the frequency band (dissipation) was also determined graphically, and the values were compared with the zero crossings obtained for the same conditions. It was expected that the zero crossings would be related to the square root of the integral of the second moment of the power spectra, and Fig. 29 indicates that relatively good agreement was obtained. Thus the measured zero crossings provide some useful information concerning the dissipation, and in general are measured with considerably less effort, as frequency spectra are not required.

A limited number of tests were carried out with the flush-mounted sensor in the main test channel. Two frequency spectra taken at the 16-ft station with different polymer concentrations are shown in Fig. 30. The data have been plotted as the ratio of the power spectral densities for water and polymer. The attenuation at higher frequencies is again apparent with increasing rates of polymer injection. These spectra agree qualitatively with the results reported by Johnson and Barchi [4] based on small-scale towing tests of a flat plate.

It was found that the average bridge voltage varied with time over a considerably larger range in the main channel than in the 4-in. pipe. In the case of polymer injection the increased variation was probably associated with the non-uniformity or streaking of the dyed material, as previously mentioned. Sufficient data have not been obtained in the main channel to establish the validity of the probe as a shear-measuring device on the basis of either average bridge voltage or zero crossings.

Attempts at measuring the zero crossing rate were not entirely successful in the main channel, and thus are not reported on here. Unfortunately, the sensor failed shortly after the tests began due to erosion of the heater element by sand particles carried in the river water. Further attempts at using the flush-mounted sensor will be made in parallel with a floating-element shear dynamometer being installed in the channel floor.

G. Velocity Profiles in the Gravity Flow 4-Inch Pipe Facility

It was noted from the experiments with the hot-film sensor in the 4-in. pipe that the pipe was not hydraulically smooth at the higher Reynolds numbers. This presented the opportunity to obtain velocity profiles during drag reduction in a pipe with natural roughness. A complete discussion of this work has been presented in [18], and thus only a brief summary is presented here.

Velocity profiles were measured for both water flows and flows of homogeneous polymer solutions at various Reynolds numbers. Data for water flow have been reduced to dimensionless forms according to the law of the wall and the velocity defect law using the shear velocity obtained from the measured axial pressure drop and are plotted in Figs. 31 and 32. In Fig. 31 the data at the lower Reynolds number indicate that the pipe is hydraulically smooth. For the higher Reynolds number the effect of roughness becomes apparent as the downward shift of u^+, the maximum shift value being about 3. This effect is not, of course, apparent in the velocity defect plot of Fig. 32, which should be independent of roughness.

The largest drag reduction with polymer additives was found at the higher Reynolds numbers, and dimensionless velocity profiles for various homogeneous polymer concentrations c_H are shown in Fig. 33 for $Re = 6 \times 10^5$. It is readily seen that the effect of polymer is to increase u^+ at a given y^+. The increase in u^+, ΔB, referenced to the water value is tabulated for reference purposes in Table I for the data in Fig. 33 as well as for data taken at several other Reynolds numbers not included here. The calculated value of ΔB from Meyer's correlation was based on a critical shear velocity of 0.131 fps obtained as a reasonable estimate from the experimental data. In nearly every instance the calculated values are greater than those measured, particularly at the lower concentrations.

The discrepancy would be still greater if a lower critical shear velocity had been used.

Table I

$Re \times 10^{-5}$	Conc. ppm	u_*, fps	ΔB_{exp}	$\Delta B_{cal.}$	Drag Reduction, per cent
3.05	0	0.373	--	--	0
	2	0.369	0.7	3.37	2.16
	4.85	0.359	1.44	5.10	7.2
	9.24	0.303	4.76	5.87	33.8
4.40	0	0.532	--	--	0
	1.98	0.508	1.5	4.37	9.17
	4.87	0.454	4.12	6.30	27.5
	9.77	0.413	6.0	8.23	40.2
6.00	0	0.710	--	--	0
	2	0.620	3.6	5.06	23.8
	5	0.534	7.4	7.22	43.6
	9.4	0.512	8.8	9.6	48.2

It should be noted that the above-mentioned differences do not appear to be associated with degradation. Samples were collected at the downstream end of the test section and compared with samples taken from the storage tank after dilution to the same concentration. The comparison was made of pressure drops as measured in the blowdown capillary rheometer, and the results were essentially identical.

IV. CONCLUSIONS

The following conclusions may be drawn relative to the character and the drag-reduction benefits of a large boundary layer injected with Polyox

WSR-301 concentrate via an axially aligned jet discharging from a continuous boundary slot:

1. For a boundary layer which was injected with Polyox near its origin, the total drag reduction was a function of the distance from the injection slot and the quantity of polymer injected into the boundary layer. At a distance of 16 ft from the slot, greater drag reduction was attained for the lower quantities injected than for the larger quantities. At further downstream distances, better drag reduction was attained with larger injection quantities. This behavior was apparently associated with more complete mixing of the injected polymer in the developing boundary layer. The maximum drag reduction of 35 per cent over about a 40-ft boundary length ($Re \sim 8 \times 10^7$) was obtained with a terminal wall concentration of about 30 ppm. This drag reduction required the injection of about 0.004 lbs/sec of polymer per unit width of channel.

2. Injection of relatively low concentrations of polymer into a thickened or partially developed boundary layer indicated that complete mixing of the polymer in the boundary layer was still attained. Further tests with larger quantities of injected polymer are required to more completely establish the trends.

3. From the limited data available, the application of anti-fouling paint to the test boundary appeared to have no serious adverse effects on the polymer's effectiveness. Some loss of effectiveness was noted for a low concentration of injected solution, but more data are needed to verify this finding.

4. When the uniformly injected polymer concentrate was color-dyed there was clear evidence that shortly after injection the flow organized into a definite pattern of large wavering parallel streaks. The streaking was probably a secondary three-dimensional vortex motion superimposed on a nominal two-dimensional flow. It is speculated that such streaking is normal in most supposedly two-dimensional flows, and further studies are recommended.

5. Velocity profiles with polymer injection are fuller than profiles with water alone. Boundary layer parameters, such as displacement and momentum thickness, have been reduced by the presence of the polymer. The ΔB shift of the plotted dimensionless velocity profile was difficult to establish with accuracy; however, the values obtained appear to be somewhat lower than those found in smooth pipe flows of homogeneous solutions.

6. Profiles of the concentration of the polymer in the boundary layer may be adequately sensed by adding a measurable tracer material to the injected concentrate. The presence of the fluorescent tracer material in withdrawal samples was readily evaluated using standard fluorimeter techniques. The flow streaking described in Conclusion Item 4 necessitated long sample withdrawal times to allow adequate averaging. Concentration profiles were dimensionally correlated with suitable parameters for low quantities of polymer injected into the boundary layer. As the quantity of polymer was increased, the correlation deteriorated at the location closest to the injection slot. Fair success was also attained in a comparison of data with predicted values of the concentration at the boundary.

7. A calibration of a flush-mounted hot-film sensor mounted in a 4-in.-diameter pipe was made. The power supplied to the probe to maintain a ten per cent overheat ratio was proportional to the cube root of the wall shear stress. For polymer flows the heat transfer was altered, as reflected by a change in the calibration. Zero crossings of the fluctuating signal from the sensor were correlated with the square root of the wall shear stress for flow in the 4-in. pipe facility and also in a rotating drum facility at much higher shear stresses. Addition of polymer to the flow had only a minor effect on the zero crossings' calibration values. The technique appears to offer a potent new tool for the measurement of boundary shear in laboratory and prototype studies. Further tests are under way.

8. Velocity profiles measured in the 4-in. pipe for various drag reductions associated with homogeneous flows of Polyox solutions indicated a smaller ΔB shift than predicted by Meyer's correlation. At the higher Reynolds numbers the pipe boundary functioned as a "rough" surface, and yet drag reductions of up to 60 per cent were obtained with homogeneous concentrations of Polyox WSR-301 of about 20 ppm.

LIST OF REFERENCES

[1] Polymers for Sewer Flow Control, Water Pollution Control Series WP-20-22, U.S. Dept. of Interior, Federal Water Pollution Control Administration, August 1969.

[2] Tsai, F. Y., "The Turbulent Boundary Layer in the Flow of Dilute Solutions of Linear Macromolecules," Doctoral Thesis, University of Minnesota, December 1968.

[3] Vogel, W. M. and Patterson, A. M., "An Experimental Investigation of the Effect of Additives Injected into the Boundary Layer of an Underwater Body," Fifth Symposium on Naval Hydrodynamics, Ship Motion and Drag Reduction, Sept. 10-12, 1964, Bergen, Norway, pp. 995-997.

[4] Johnson, B. and Barchi, R. H., "Effect of Drag-Reducing Additives on Boundary Layer Turbulence," Journal of Hydronautics, Vol. 2, No. 3, July 1968, pp. 168-175.

[5] Wu, Jin, "Drag Reduction in External Flows of Additive Solutions," Viscous Drag Reduction, C. S. Wells, Editor, Plenum Press, New York, 1969, pp. 331-350.

[6] Ripken, J. F.; Wetzel, J. M.; and Killen, J. M., Drag Reduction Studies with Polymer Boundary Injection on a Large Flowing Stream, University of Minnesota, St. Anthony Falls Hydraulic Laboratory External Memorandum No. M-115, July 1968.

[7] Wetzel, J. M.; Ripken, J. F.; and Killen, J. M., The Influence of Polymer Injection on a Large-Scale Boundary Layer, University of Minnesota, St. Anthony Falls Hydraulic Laboratory External Memorandum No. M-117, May 1969.

[8] Wetzel, J. M.; Almo, J. A.; and Killen, J. M., "Turbulence Measurements in Dilute Polymer Flows," Symposium on Turbulence Measurements in Liquids, University of Missouri, Rolla, Mo., Sept. 8-9, 1969 (In Press).

[9] Wetzel, J. M. and Tsai, F. Y., "Impact Tube Measurements in Dilute Polymer Solutions," AIChE Journal, Vol. 14, No. 4, July 1968, pp. 663-664.

[10] Goren, Y.; Kane, P. O.; and Norbury, J. F., A Method of Measuring the Concentration of Certain Polymers in Dilute Aqueous Solutions, Aeronautical Research Council Report ARC 27282, September 21, 1965.

[11] Goren, Y. and Norbury, J. F., "Turbulent Flow of Dilute Aqueous Polymer Solutions," Journal of Basic Engineering, Transactions, ASME, Vol. 89, No. 4, December 1967, pp. 814-822.

[12] Ruch, J. E.; Taylor, E. J.; and Yarborough, V. A., "The Direct Determination of Small Amounts of High-Molecular-Weight Poly (Ethylene Oxide) in Beer," Annual Proceedings of American Brewing Chemists, 1965, pp. 170-175.

[13] Clauser, F. H., "Turbulent Boundary Layers in Adverse Pressure Gradients," Jour. Aeronautical Science, Vol. 21, No. 2, February 1954, pp. 91-108.

[14] Poreh, M. and Cermak, J. E., "Study of Diffusion from a Line Source in a Turbulent Boundary Layer," International Journal of Heat and Mass Transfer, Vol. 7, 1964, pp. 1083-1095.

[15] Morkovin, M. V., "On Eddy Diffusivity, Quasi-Similarity and Diffusion Experiments in Turbulent Boundary Layers," International Journal of Heat and Mass Transfer, Vol. 8, 1965, pp. 129-145.

[16] Fabula, A. G. and Burns, T. J., "Dilution in a Turbulent Boundary Layer with Polymeric Friction Reduction," Paper presented at AIAA 2nd Advanced Marine Vehicles and Propulsion Meeting, Seattle, Wash., May 21-23, 1969; also Naval Undersea Research and Development Center TP 171, April 1970.

[17] White, Frank M., "An Analysis of Flat-Plate Drag with Polymer Additives," Journal of Hydronautics, Vol. 2, No. 4, October 1968, pp. 181-186.

[18] Sehgal, C. K., "Effect of Polymer on Velocity Profiles in a Commercially Rough Pipe," Master's Thesis, University of Minnesota, December 1969.

F I G U R E S

(1 through 33)

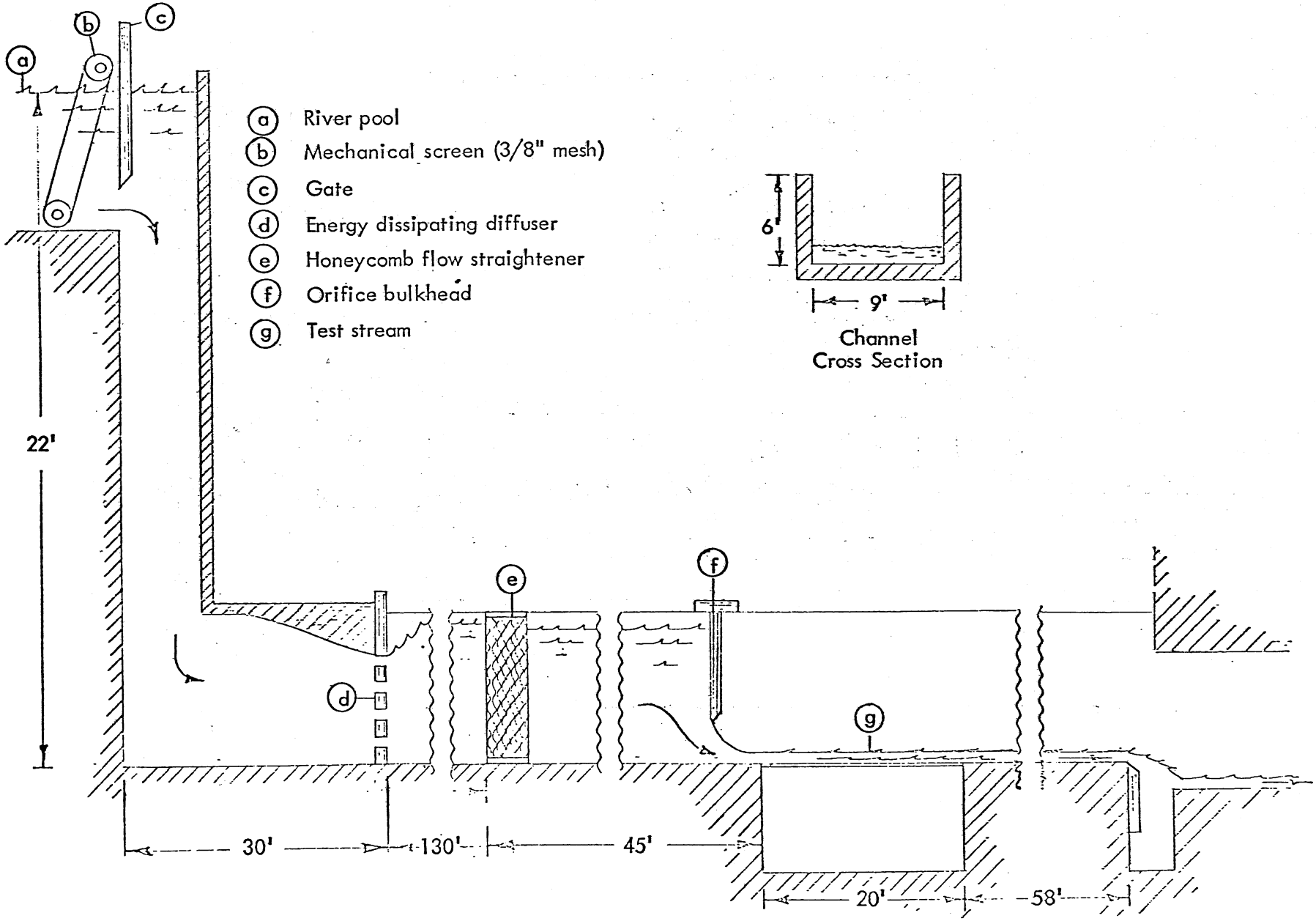

Fig. 1 - Schematic Longitudinal Elevation of Main Flow Channel

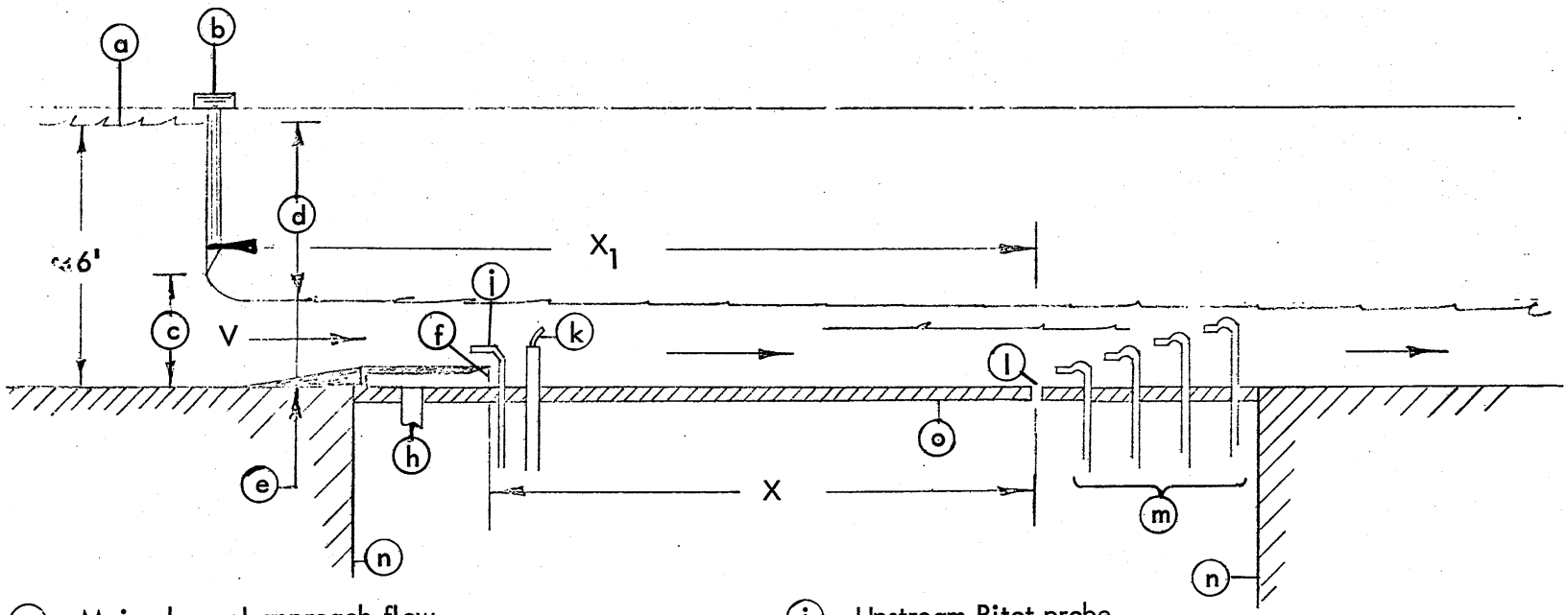

(a) Main channel approach flow
(b) Orifice bulkhead
(c) Orifice opening (two-dimen.)
(d) Differential gravity head ($h = V^2/2g$)
(e) Test stream depth
(f) Polymer Injection slot (two-dimen.)
(h) Pumped polymer supply
(j) Upstream Pitot probe
(k) Turbulence dye injector
(l) Boundary static pressure probe
(m) Combined stagnation and sample withdrawal tubes (9)
(n) Concrete structure
(o) Steel floor system

Fig. 2 - The Test Section With Pertinent Auxiliaries

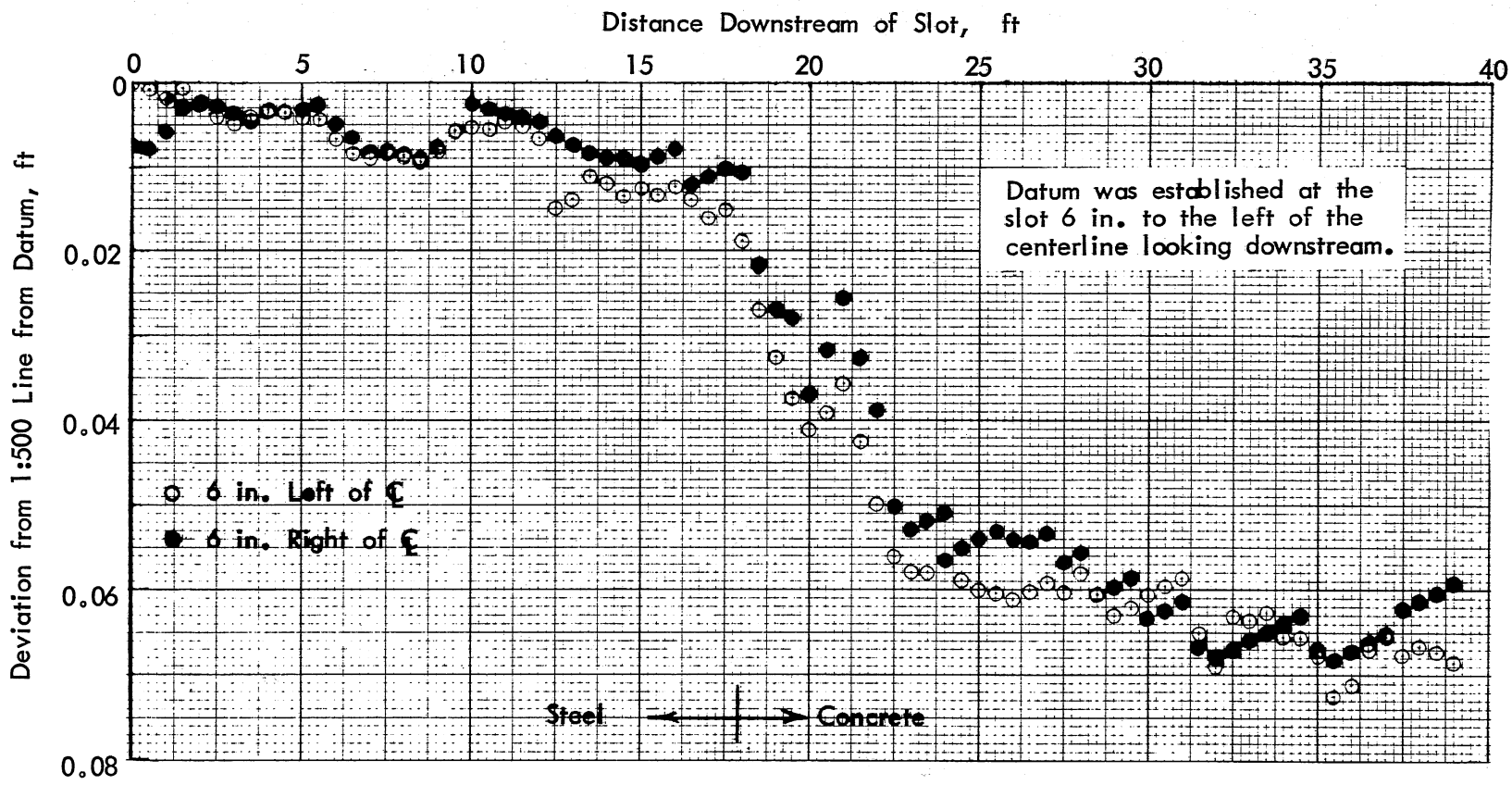

Fig. 3 - Longitudinal Profile of Channel Bottom Near Centerline

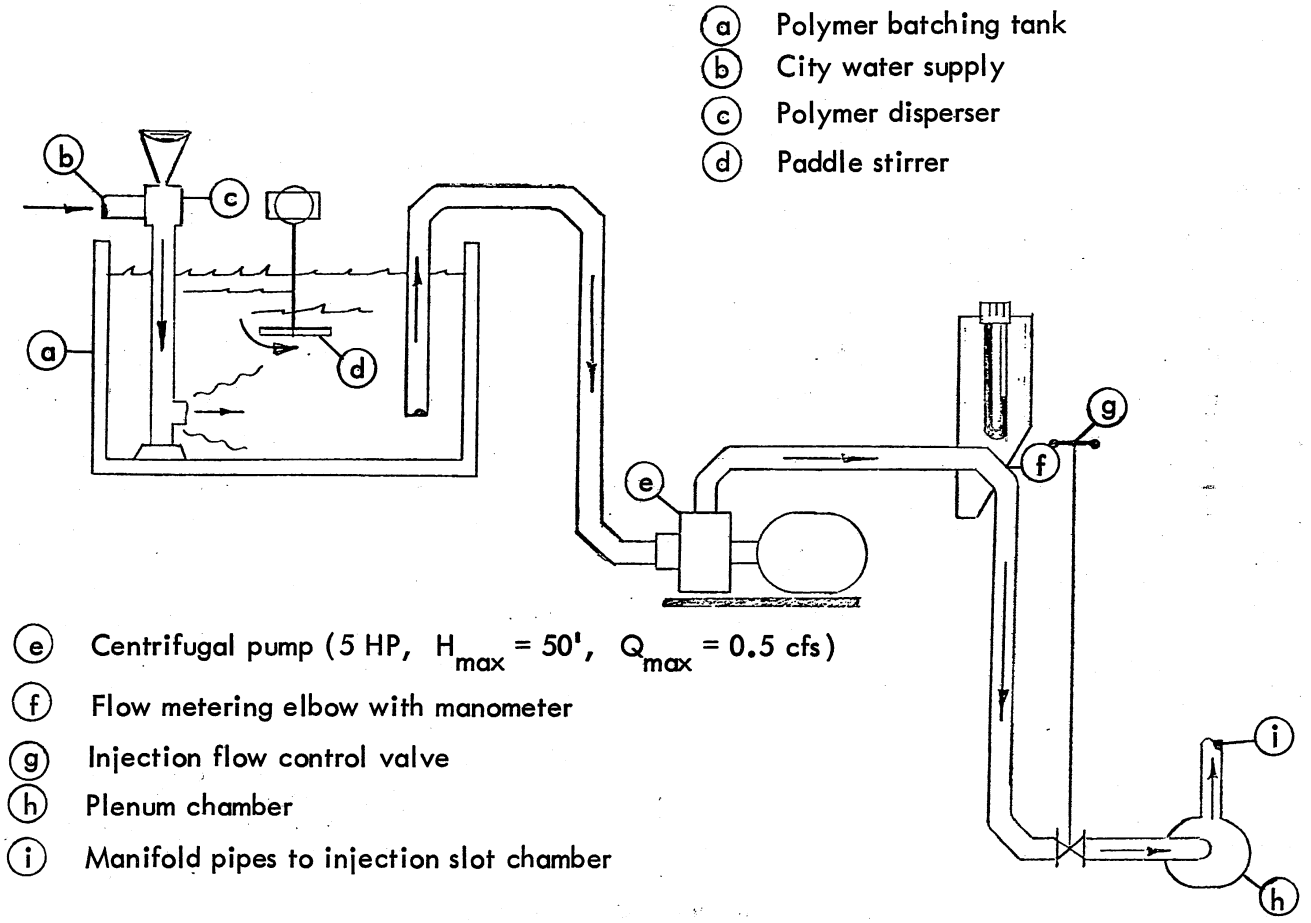

Fig. 4 - Schematic Arrangement of Polymer Mixing and Pumping System

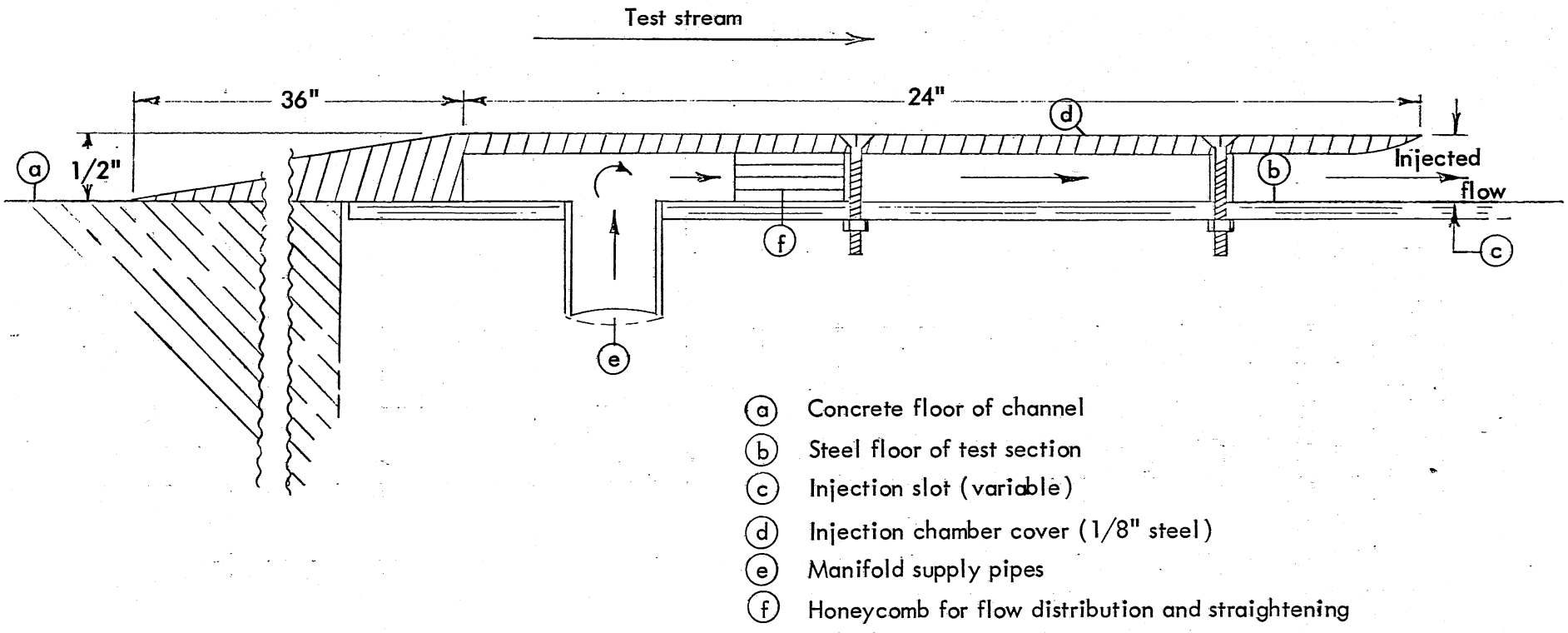

(a) Concrete floor of channel
(b) Steel floor of test section
(c) Injection slot (variable)
(d) Injection chamber cover (1/8" steel)
(e) Manifold supply pipes
(f) Honeycomb for flow distribution and straightening

Fig. 5 - The Injection Slot Assembly

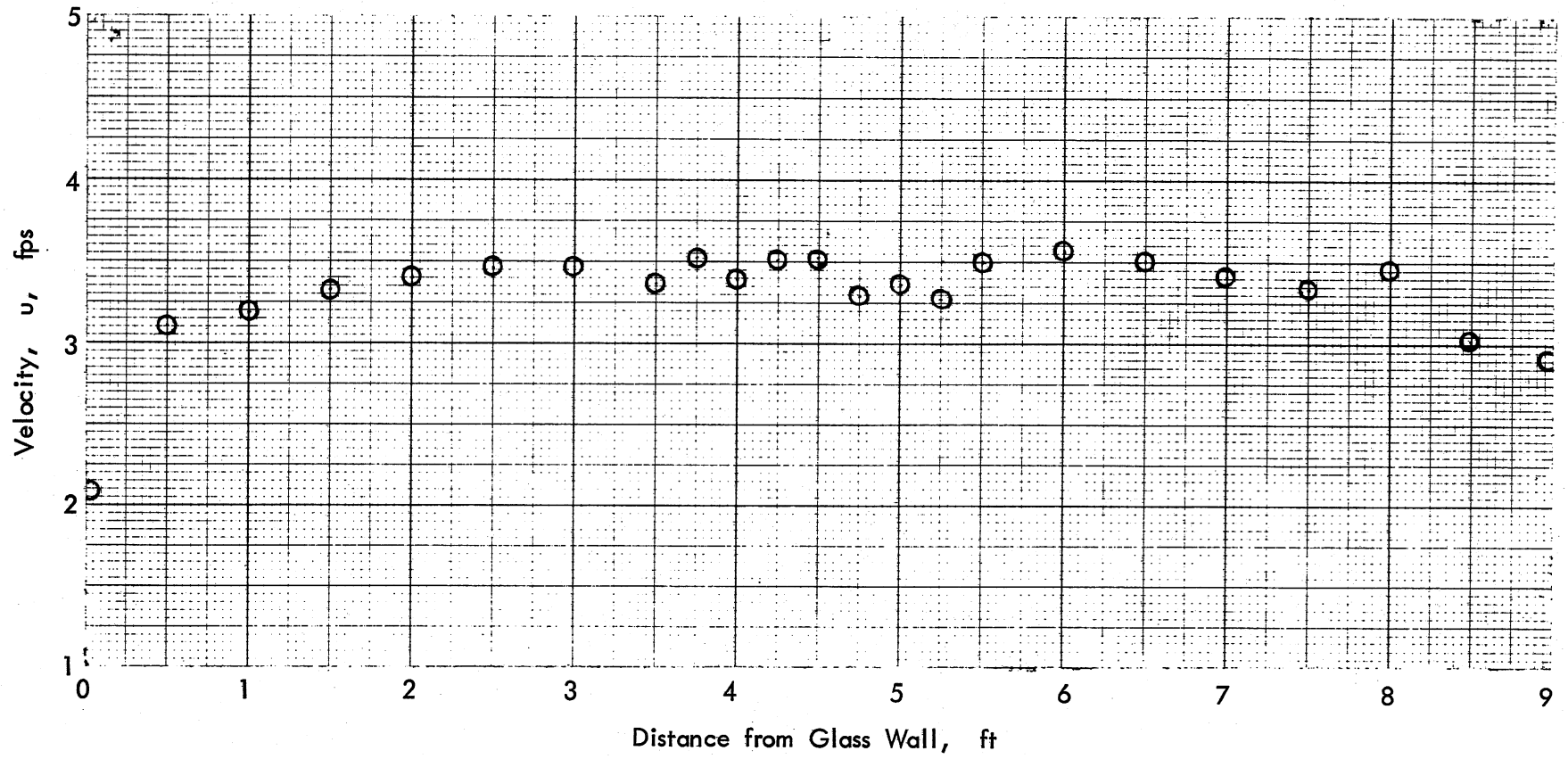

Fig. 6 - Lateral Distribution of Velocity of the Two-Dimensional Stream Issuing From the Injection Slot (Water Only)

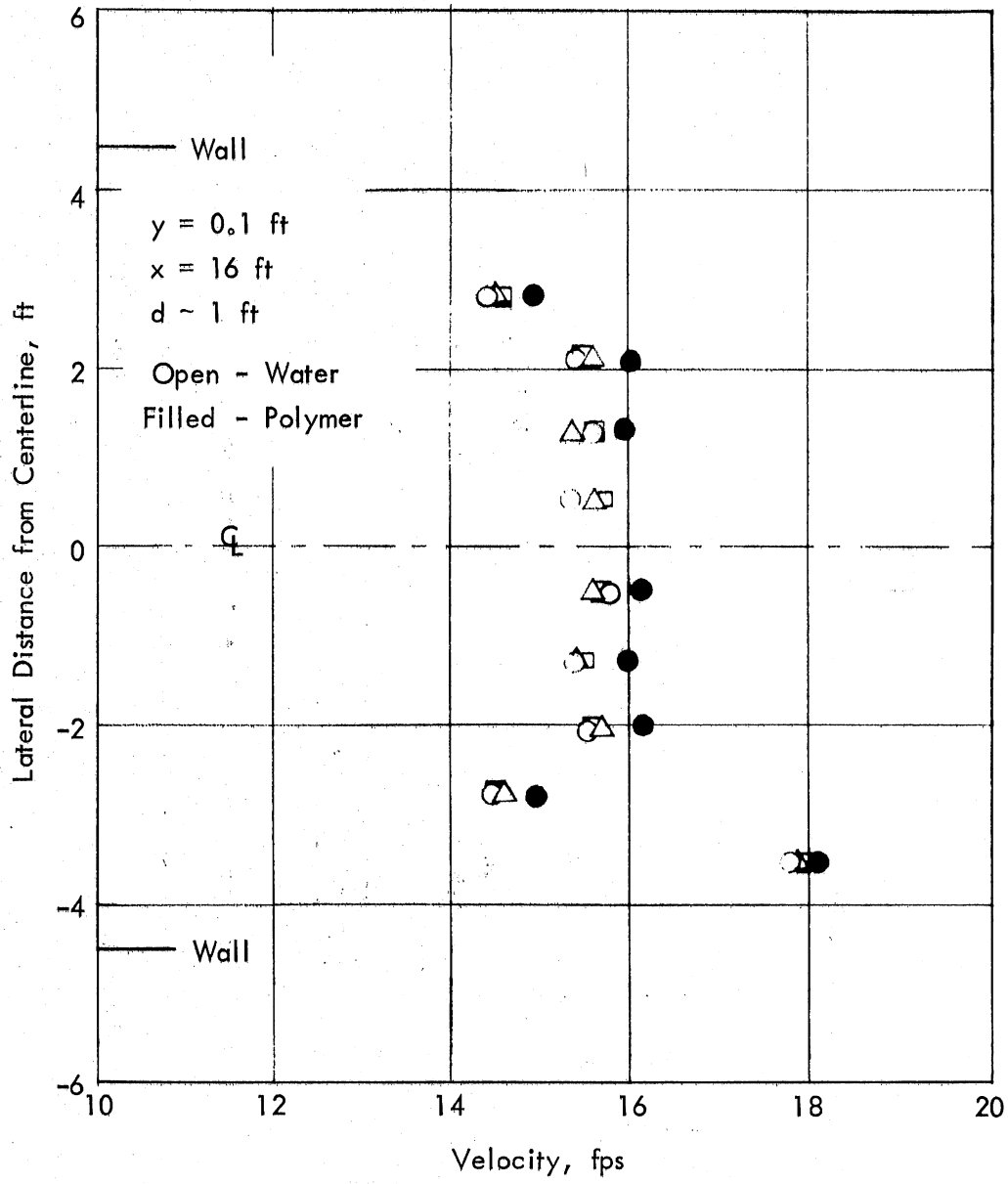

Fig. 7 - Lateral Distribution of Velocity 16 ft from the Injection Slot

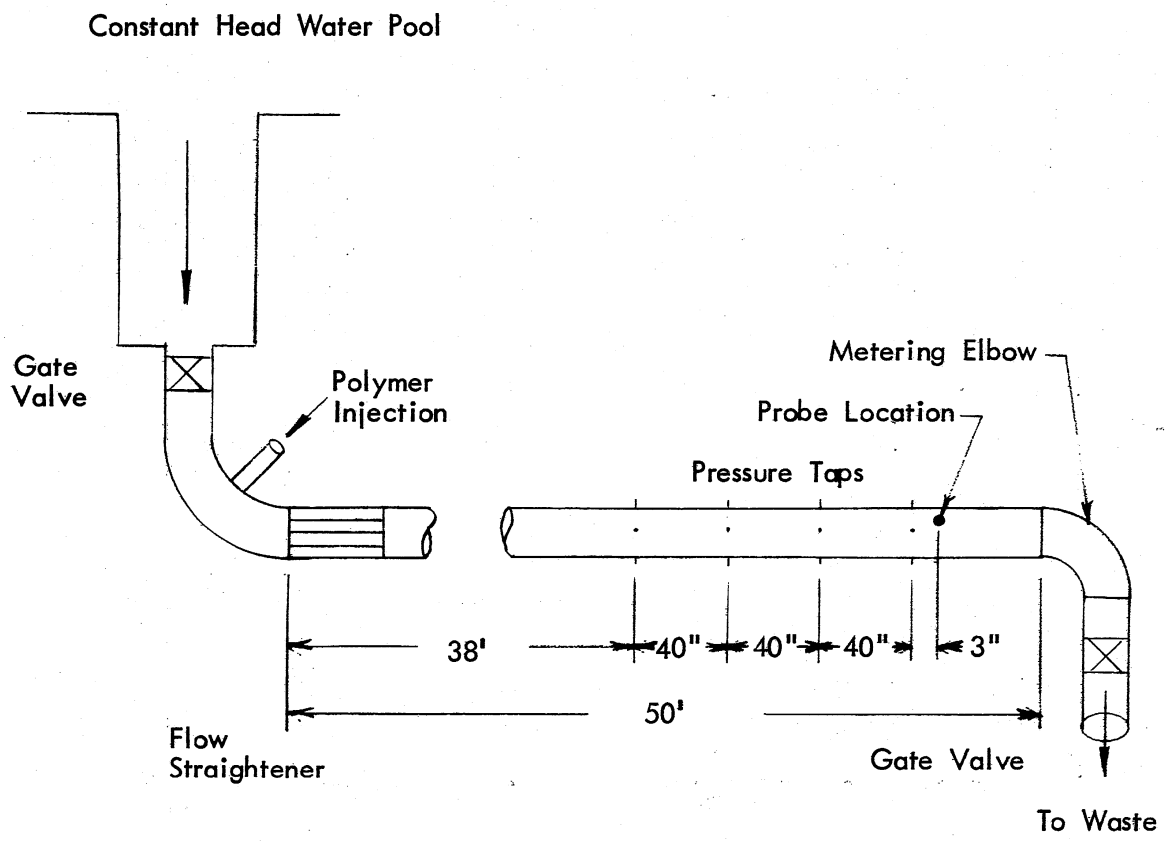

Fig. 8 - Schematic of Gravity Flow Pipe Facility

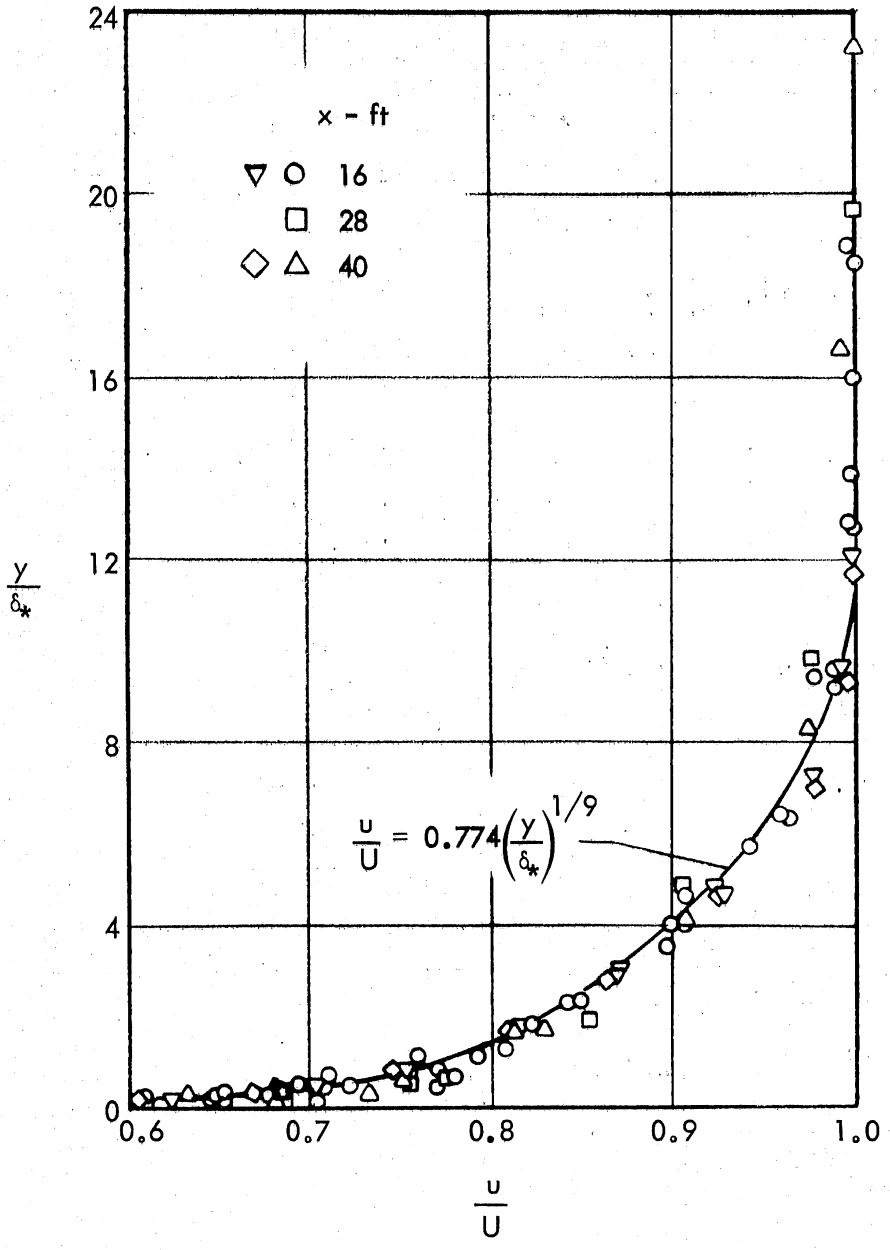

Fig. 9 - Dimensionless Velocity Profiles for Water Flow in the Main Channel

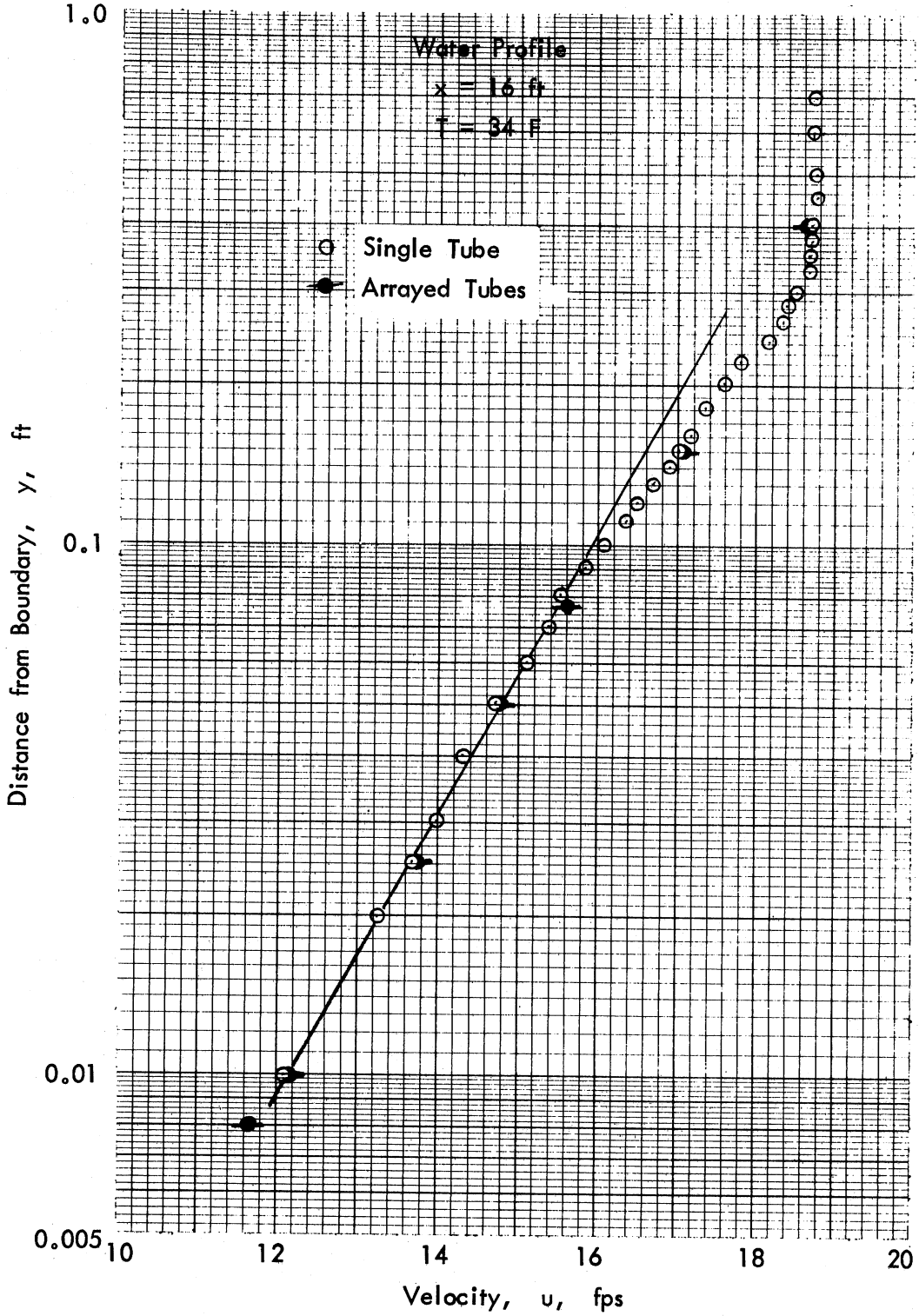

Fig. 10 - Semi-Logarithmic Velocity Profile for Water Flow in the Main Channel

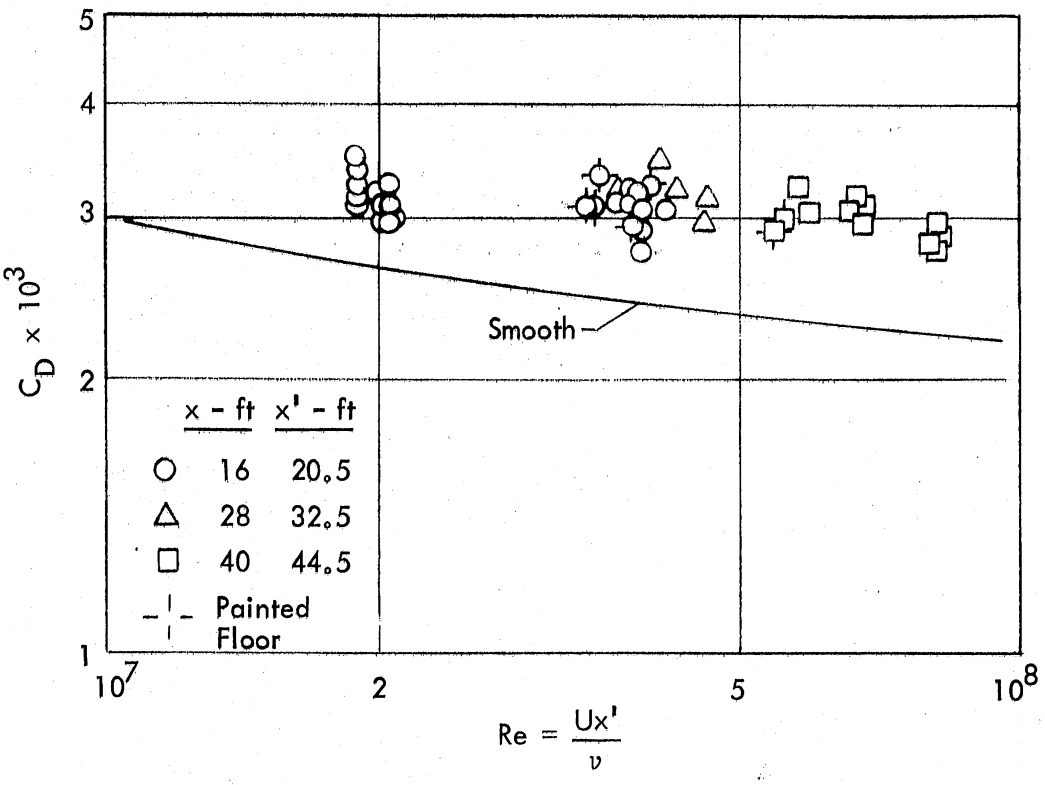

(a)

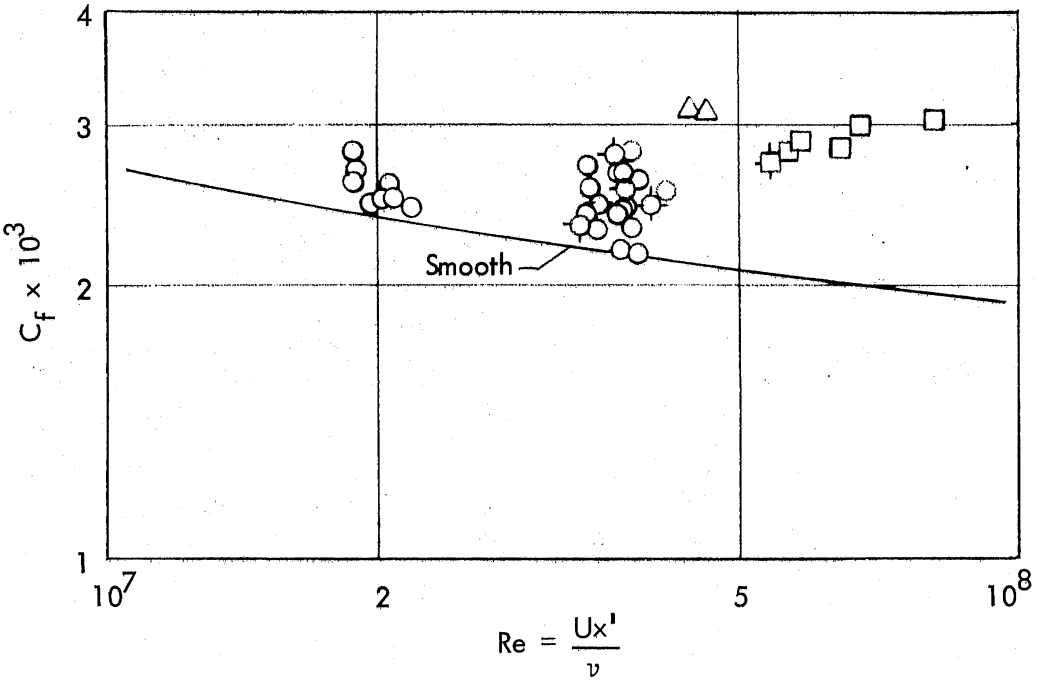

(b)

Fig. 11 - Drag Coefficients for Water Flow in the Main Channel

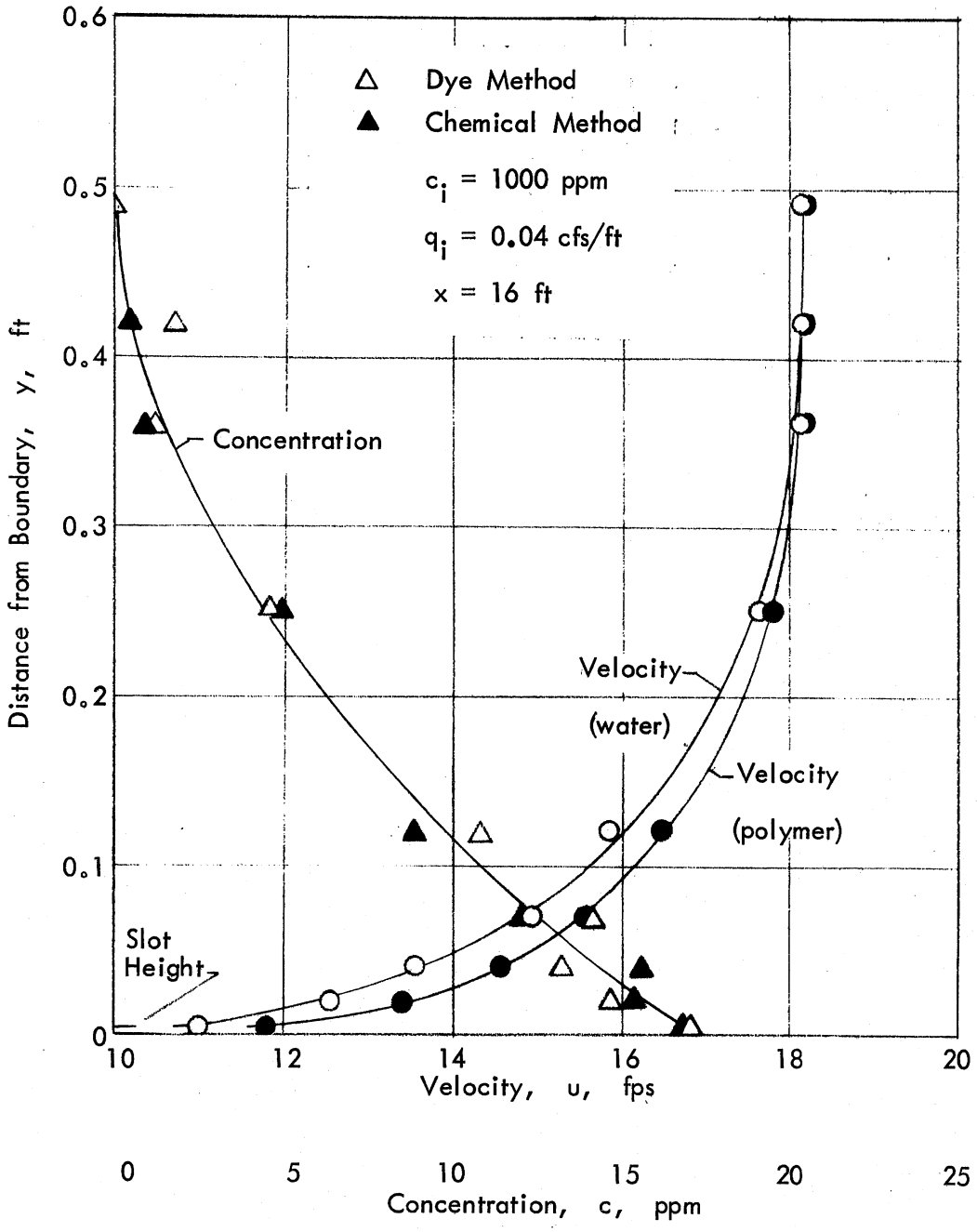

Fig. 12 - Typical Velocity and Concentration Profiles with Polymer Injection

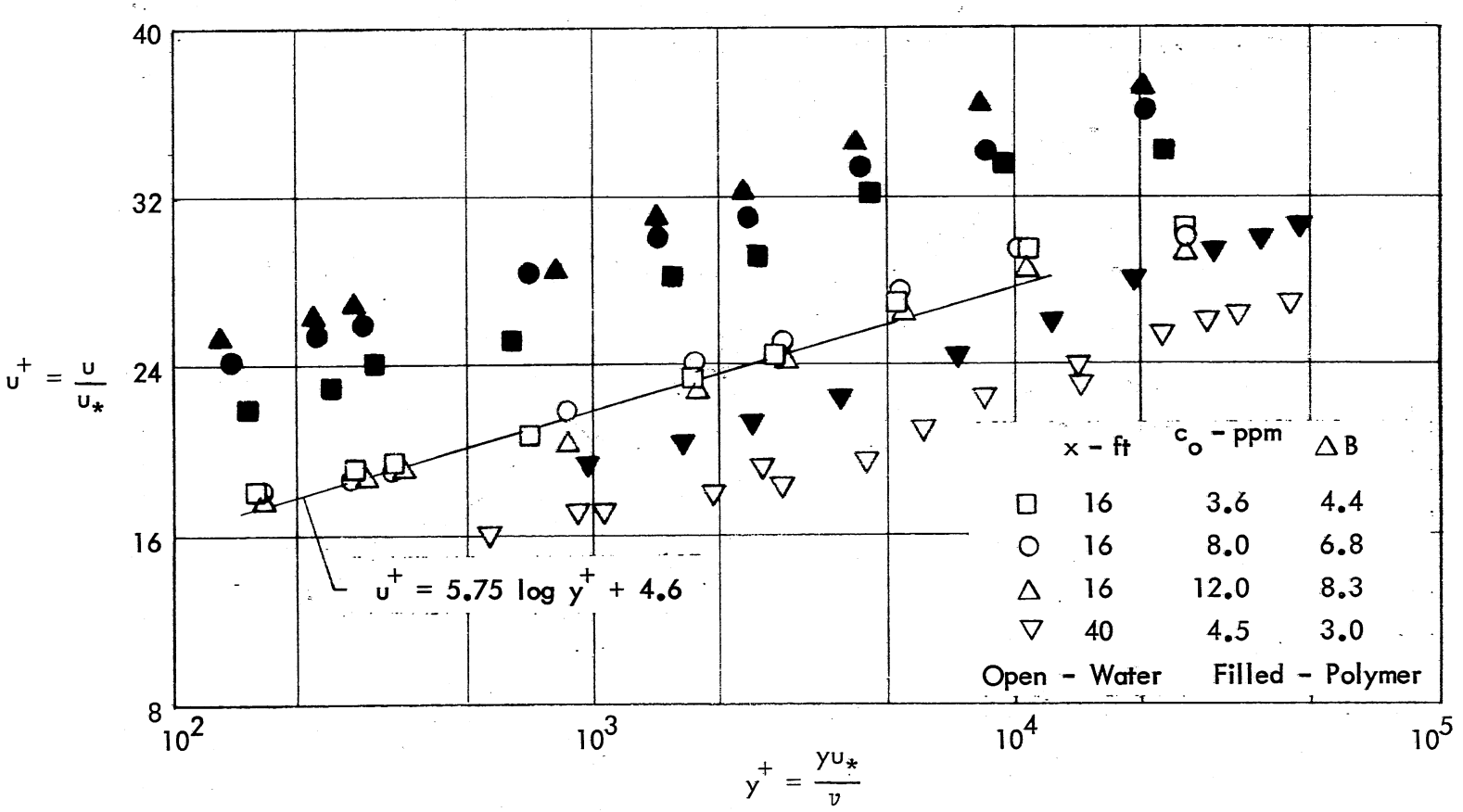

Fig. 13 - Influence of Polymer Injection on Law of the Wall

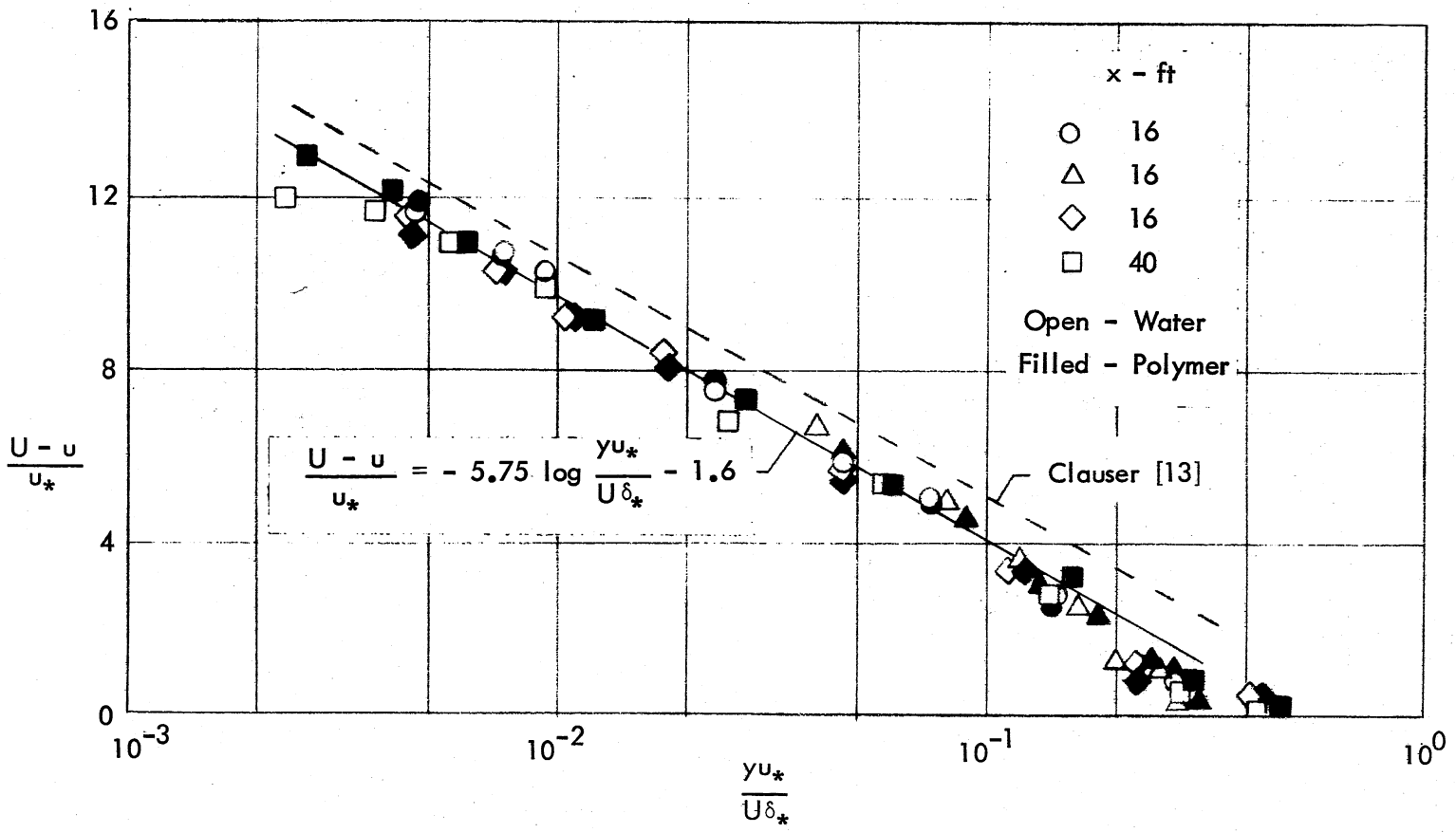

Fig. 14 - Influence of Polymer Injection on Velocity Defect

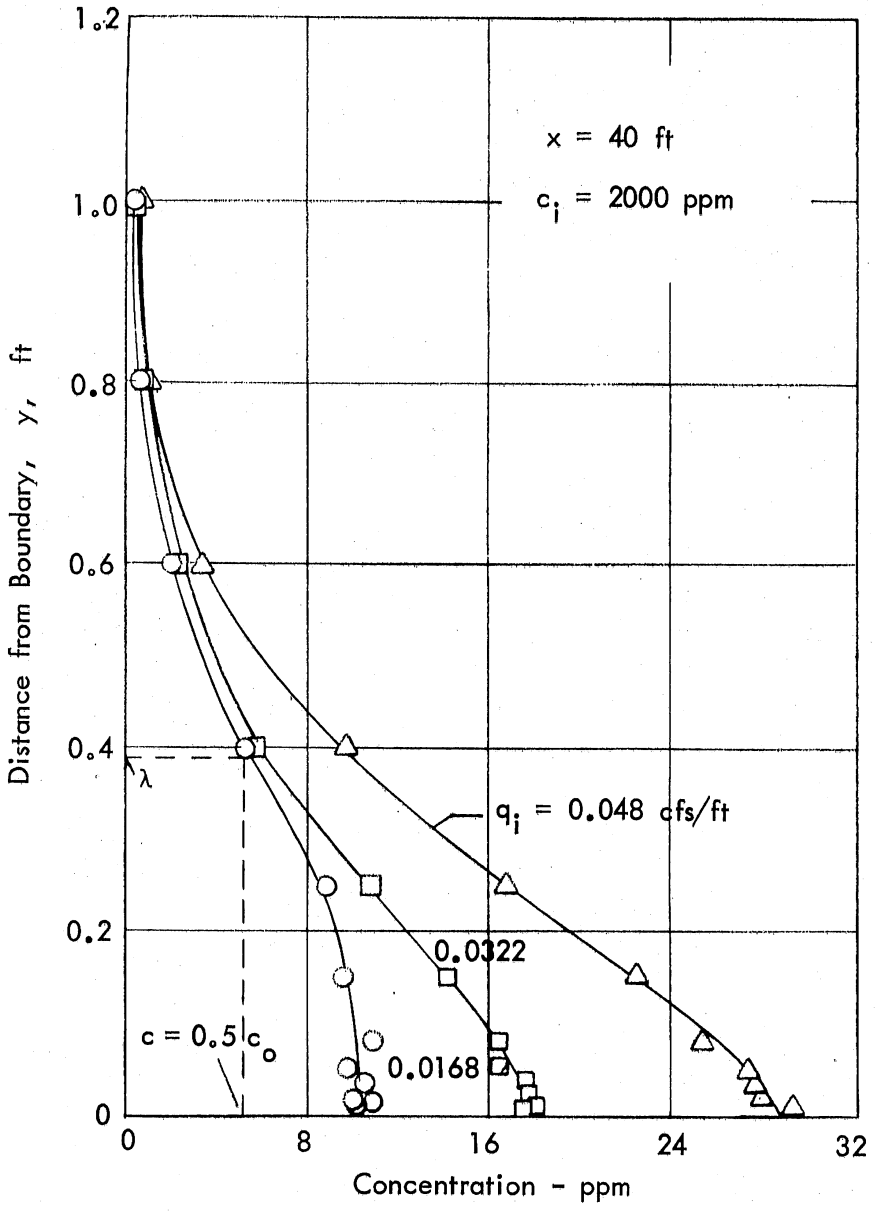

Fig. 15 - Typical Variation of Concentration Profiles with Injection Rate

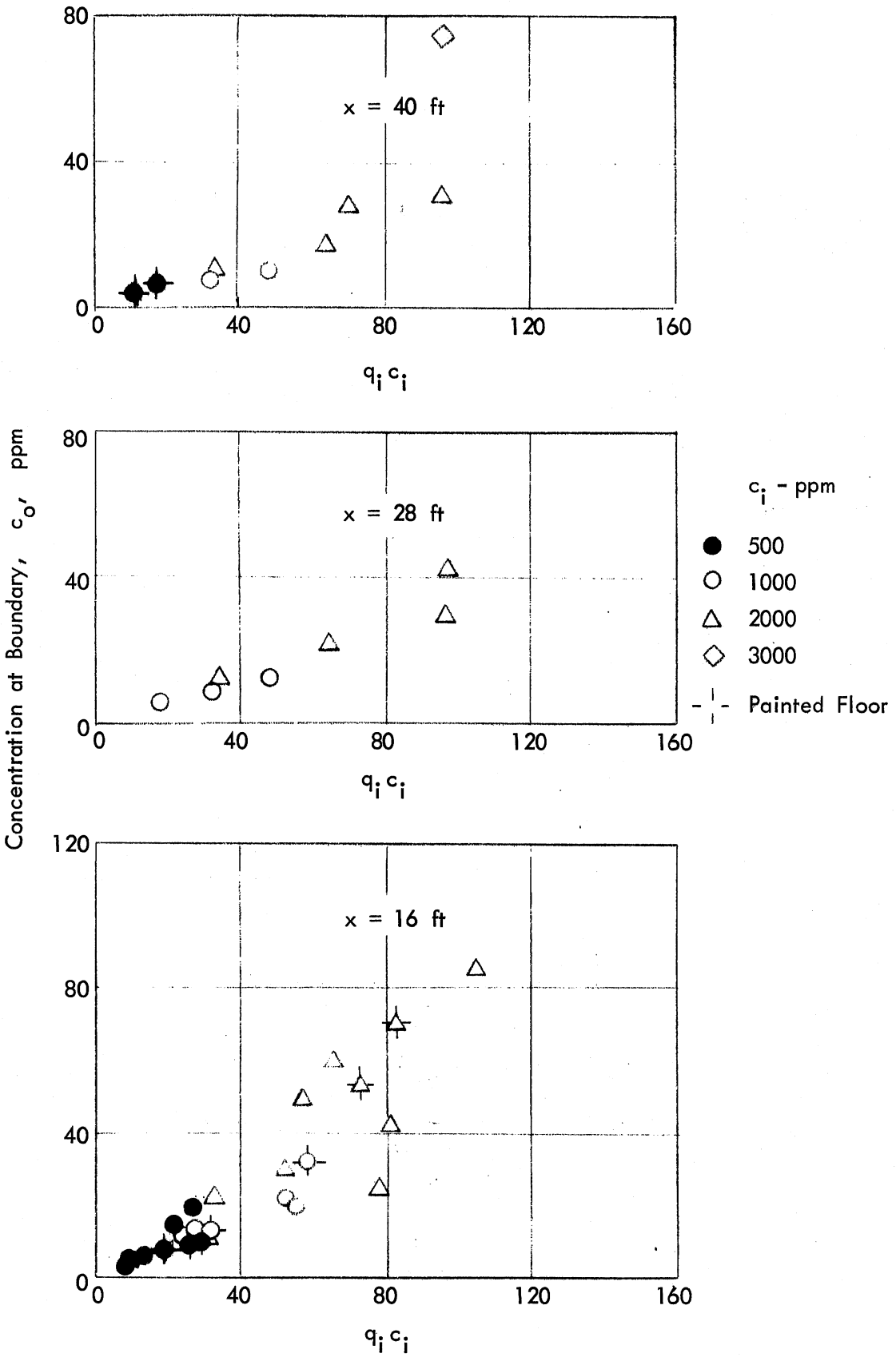

Fig. 16 - Concentration at Boundary as function of Quantity of Polymer Entering the Boundary Layer

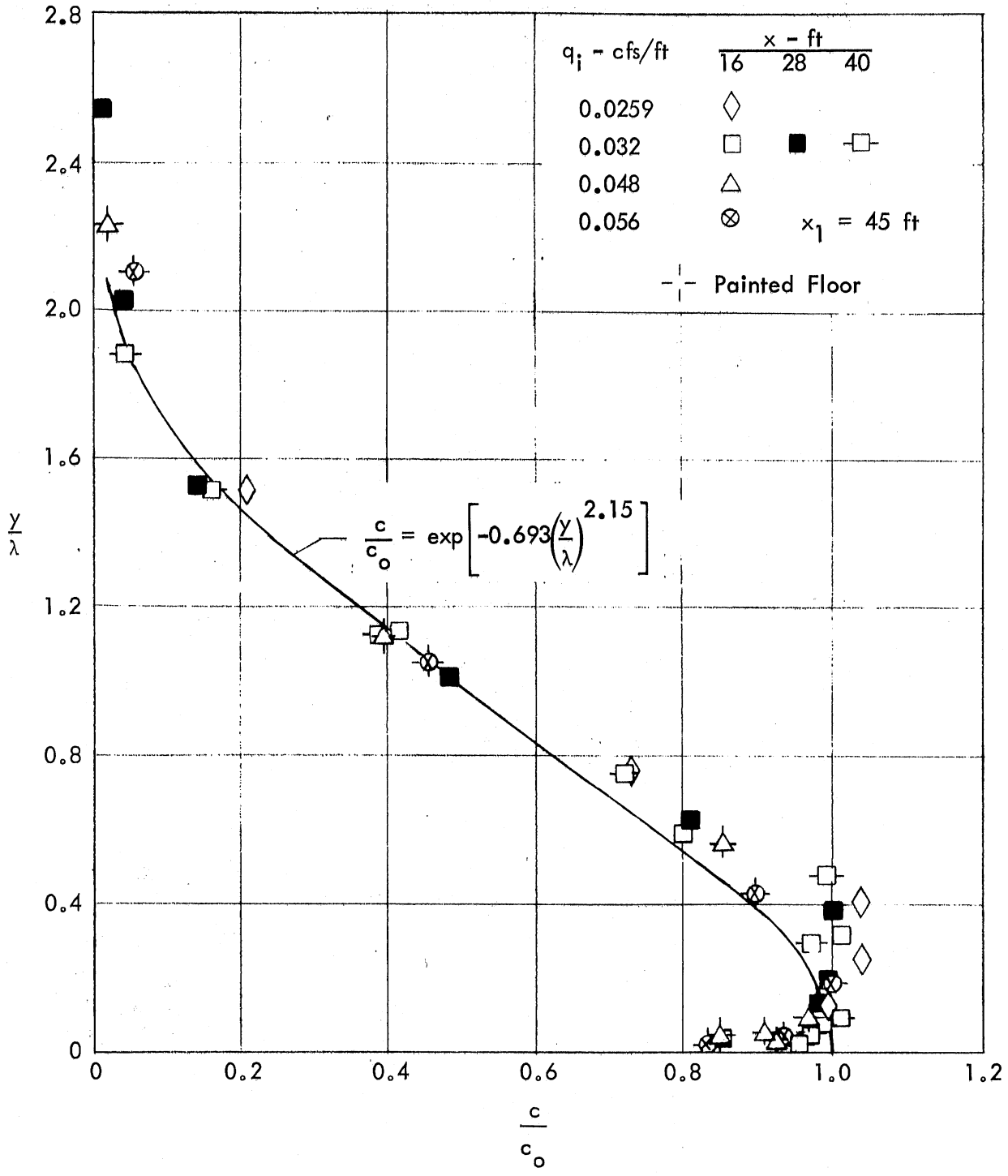

Fig. 17 - Dimensionless Concentration Profiles for Injection of Dyed Water

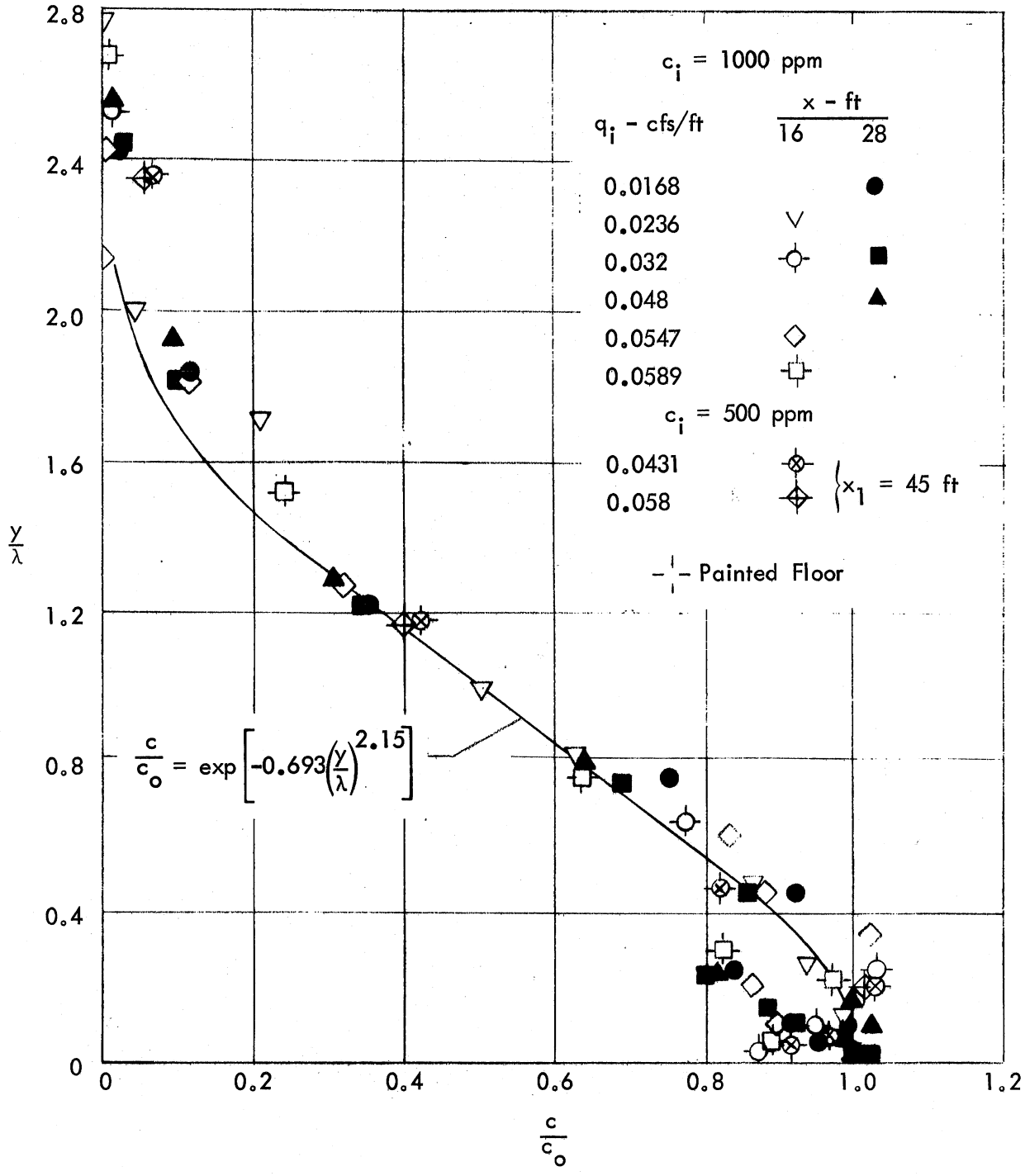

Fig. 18 - Dimensionless Concentration Profiles for Polymer Injection of Lower Concentrations

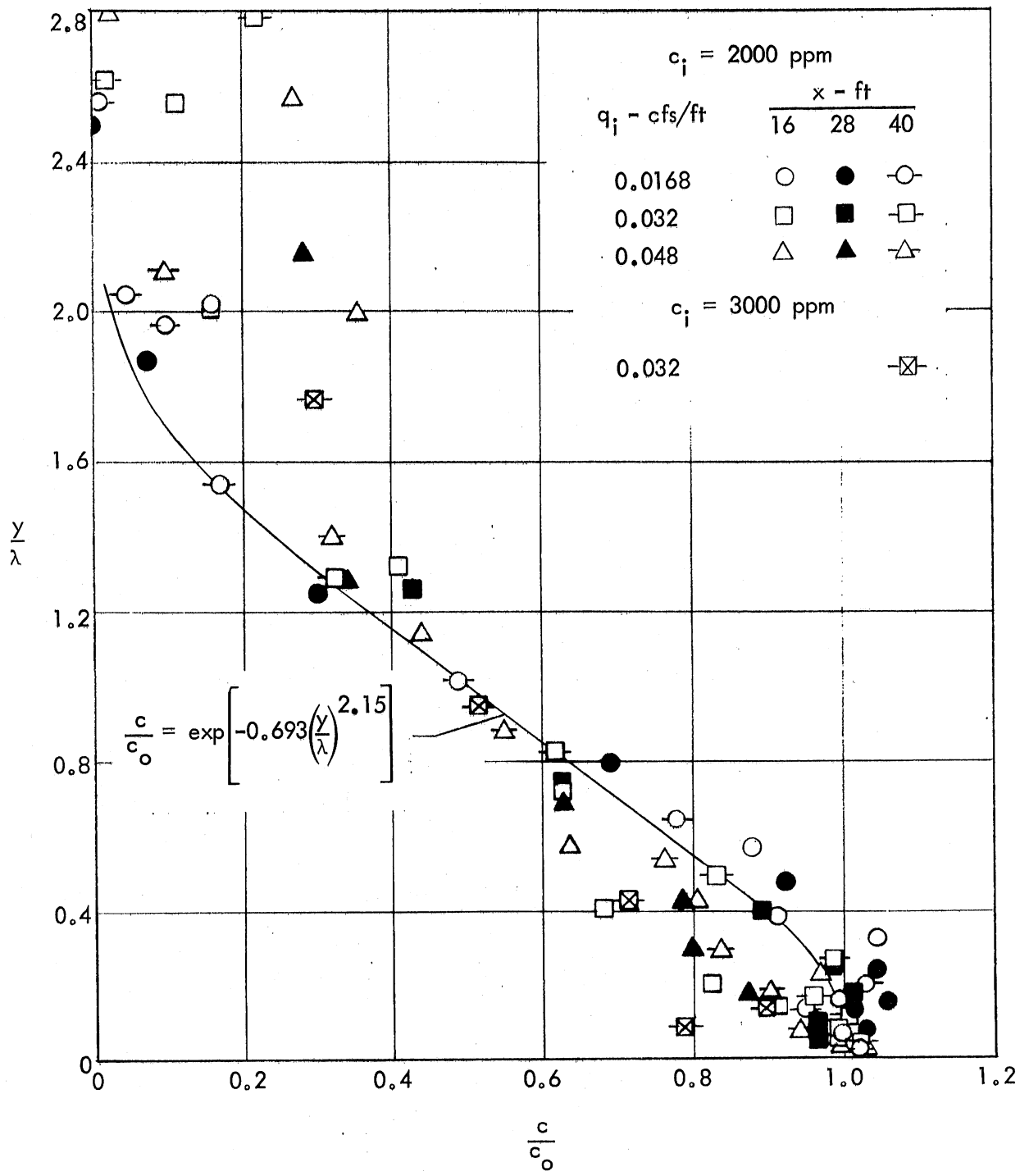

Fig. 19 - Dimensionless Concentration Profiles for Polymer Injection of Higher Concentrations

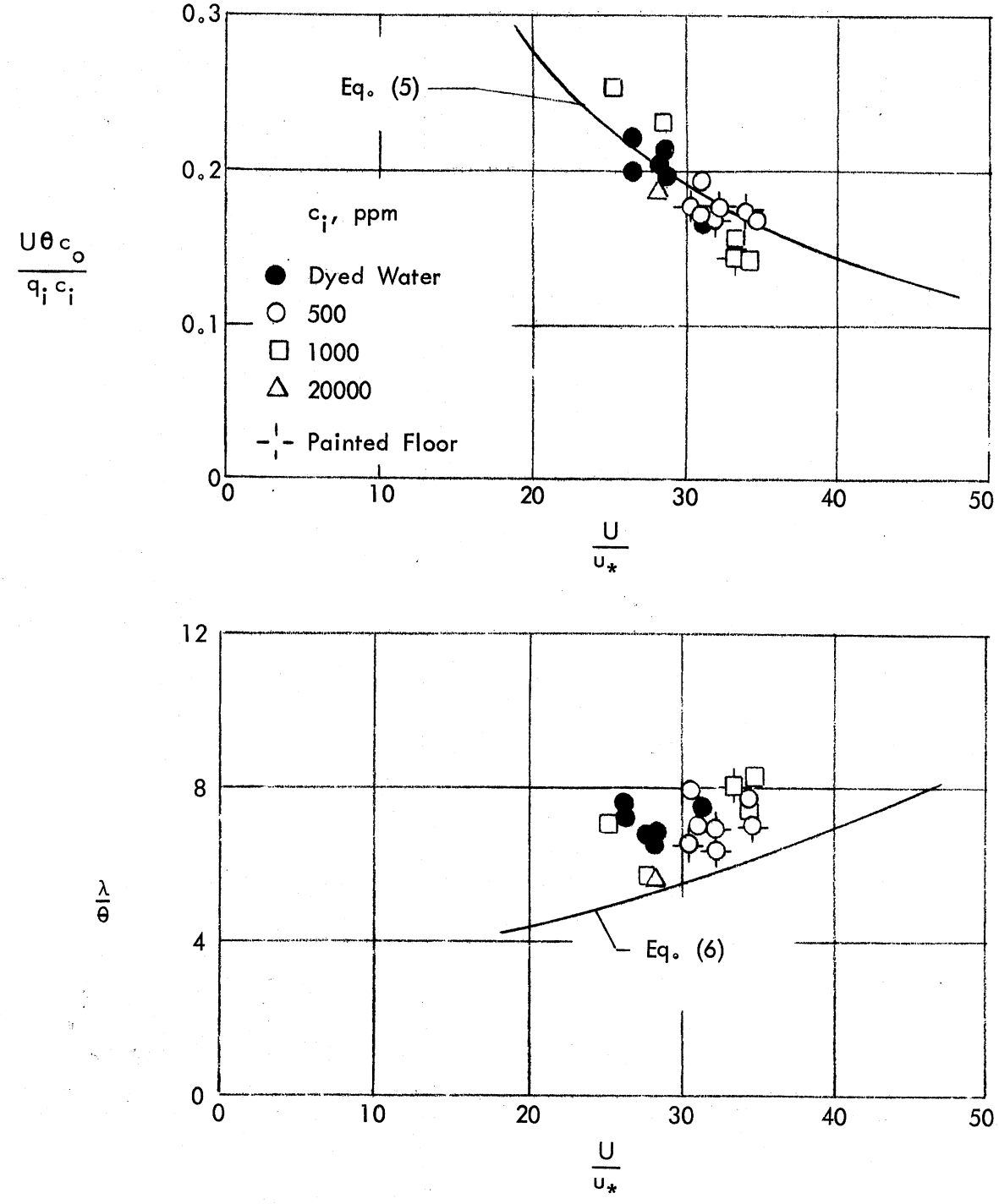

Fig. 20 - Comparison of Data with Dimensionless Scaling Parameters

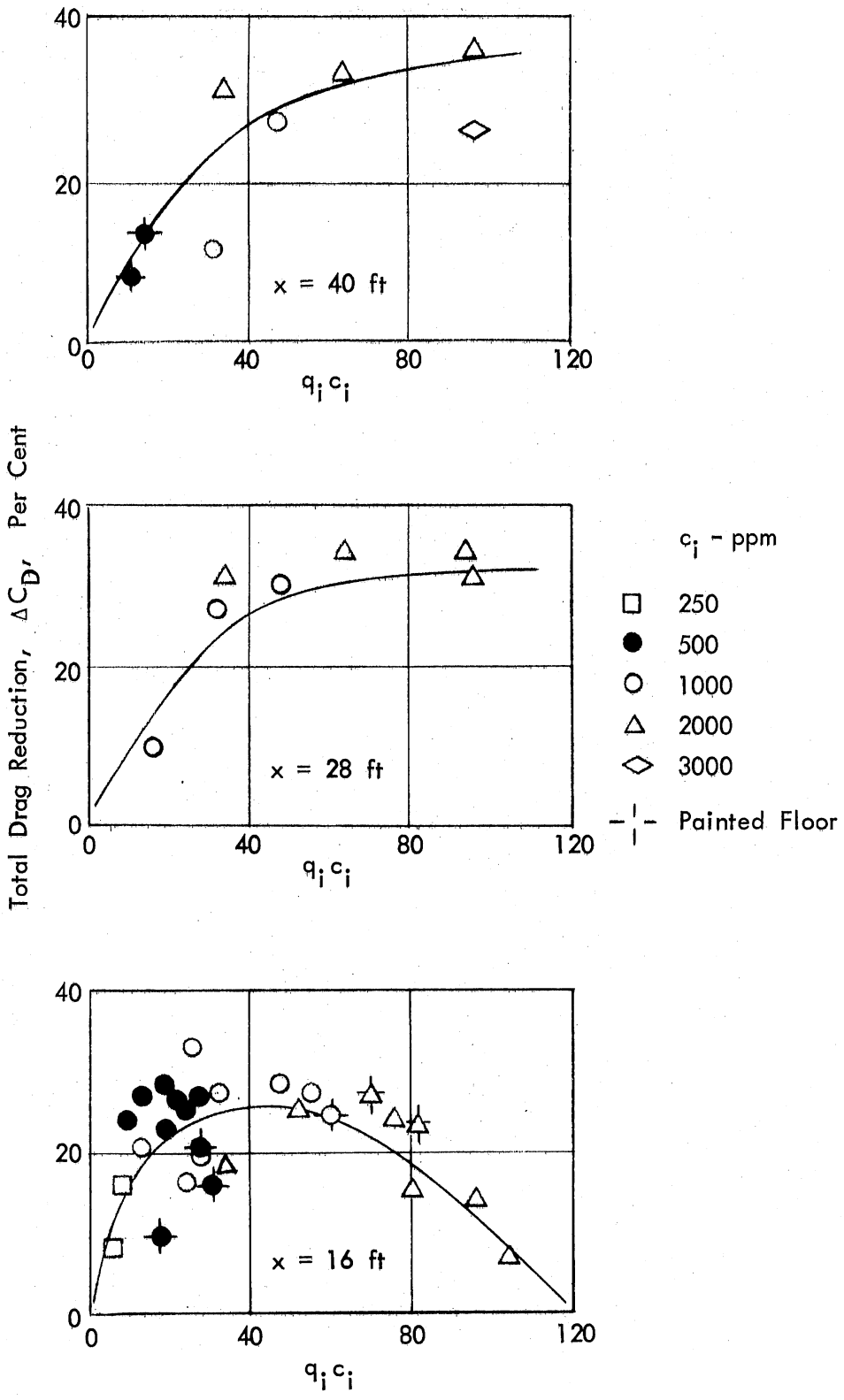

Fig. 21 - Influence of Quantity of Injected Polymer on Total Drag Reduction

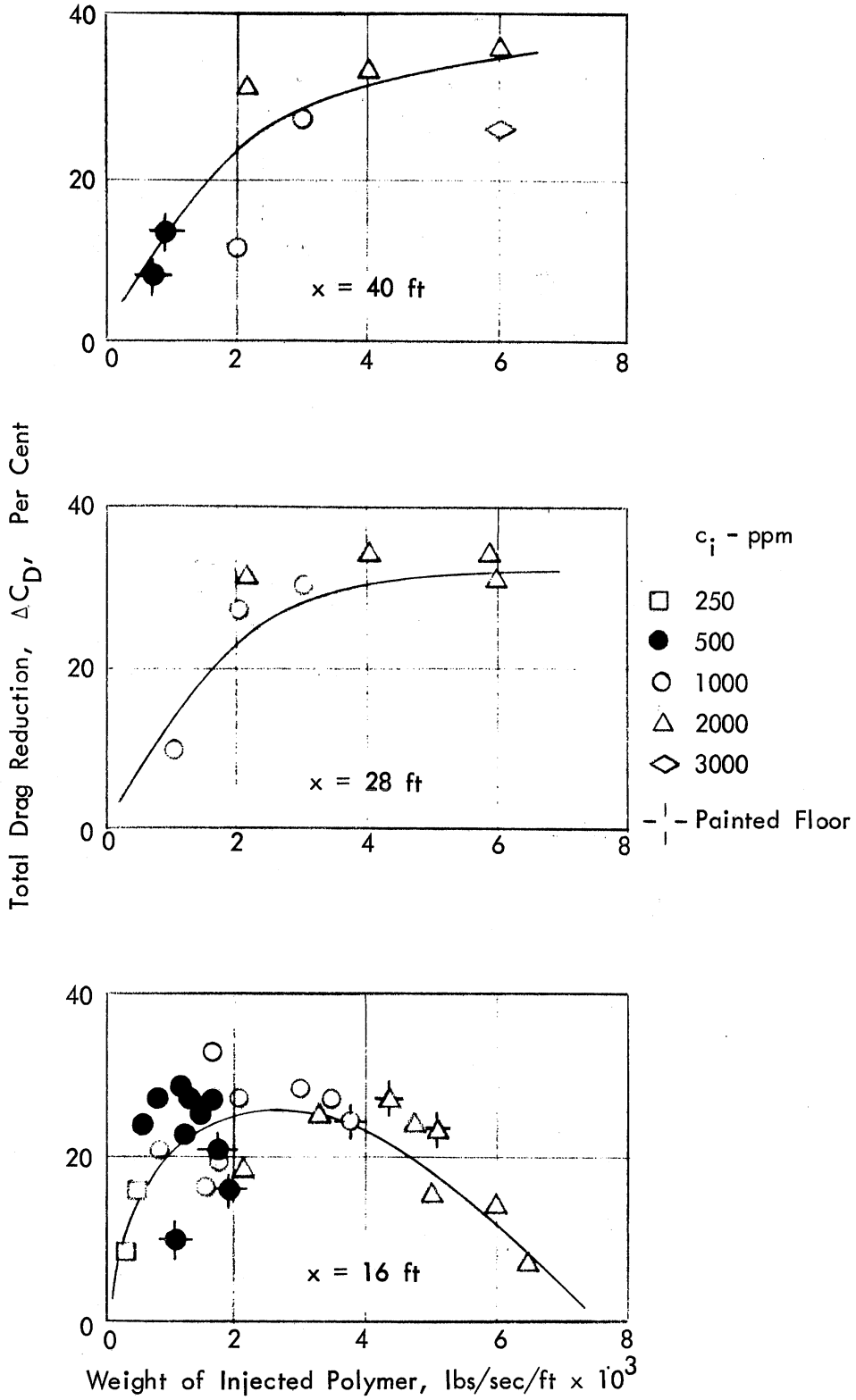

Fig. 22 - Total Drag Reduction as function of Weight of Polymer Injected per Unit Width

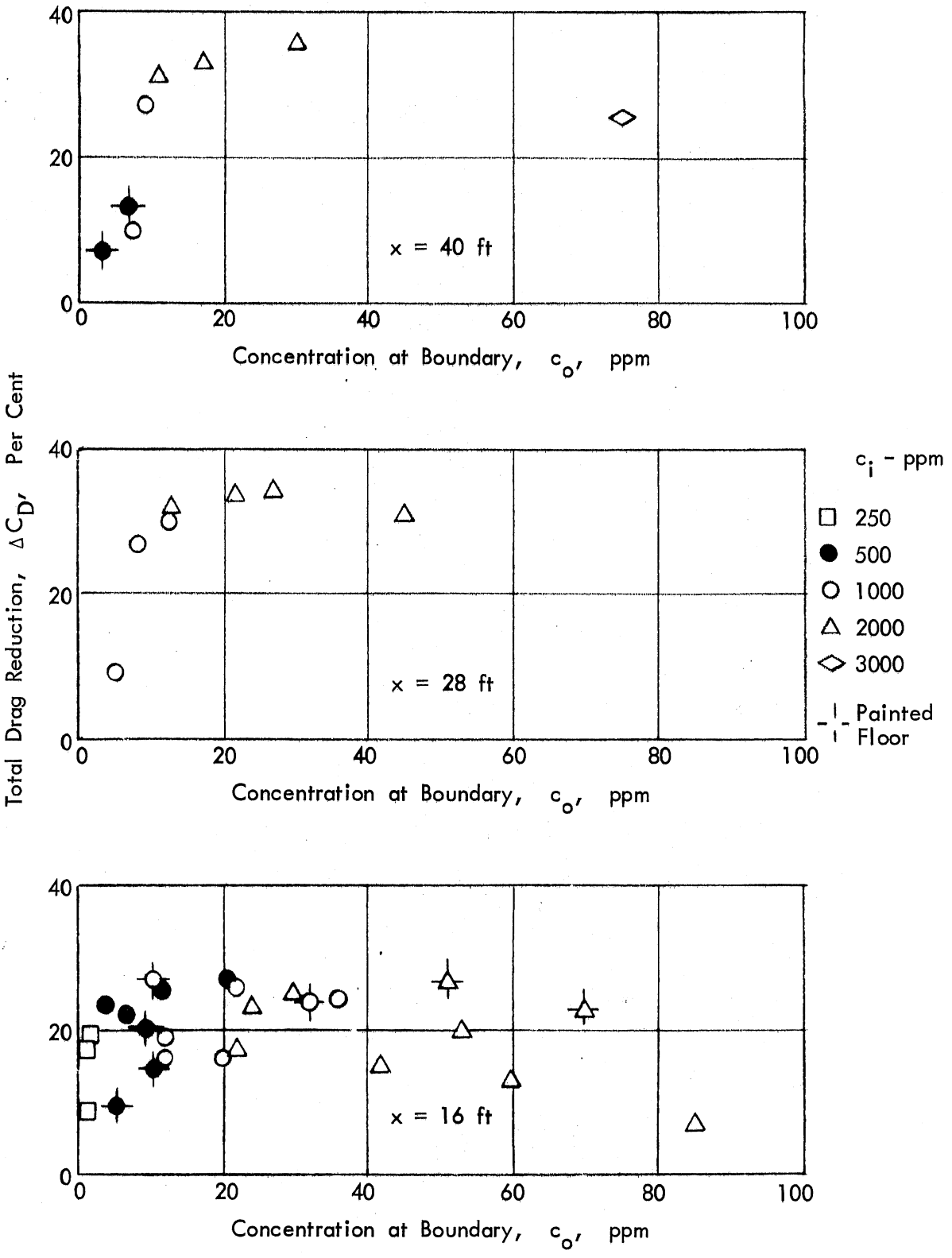

Fig. 23 - Variation of Total Drag Reduction with Concentration at the Boundary

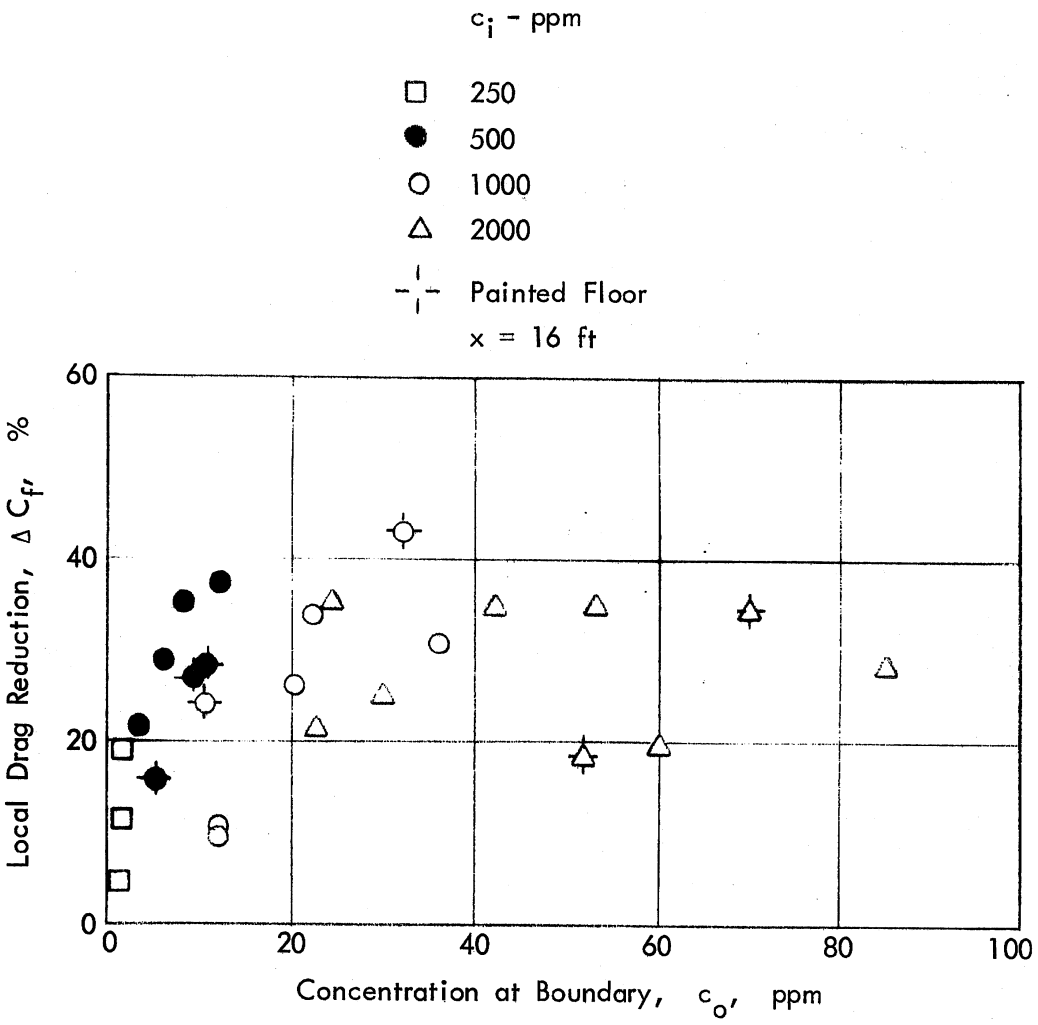

Fig. 24 - Variation of Local Drag Reduction with Concentration at the Boundary

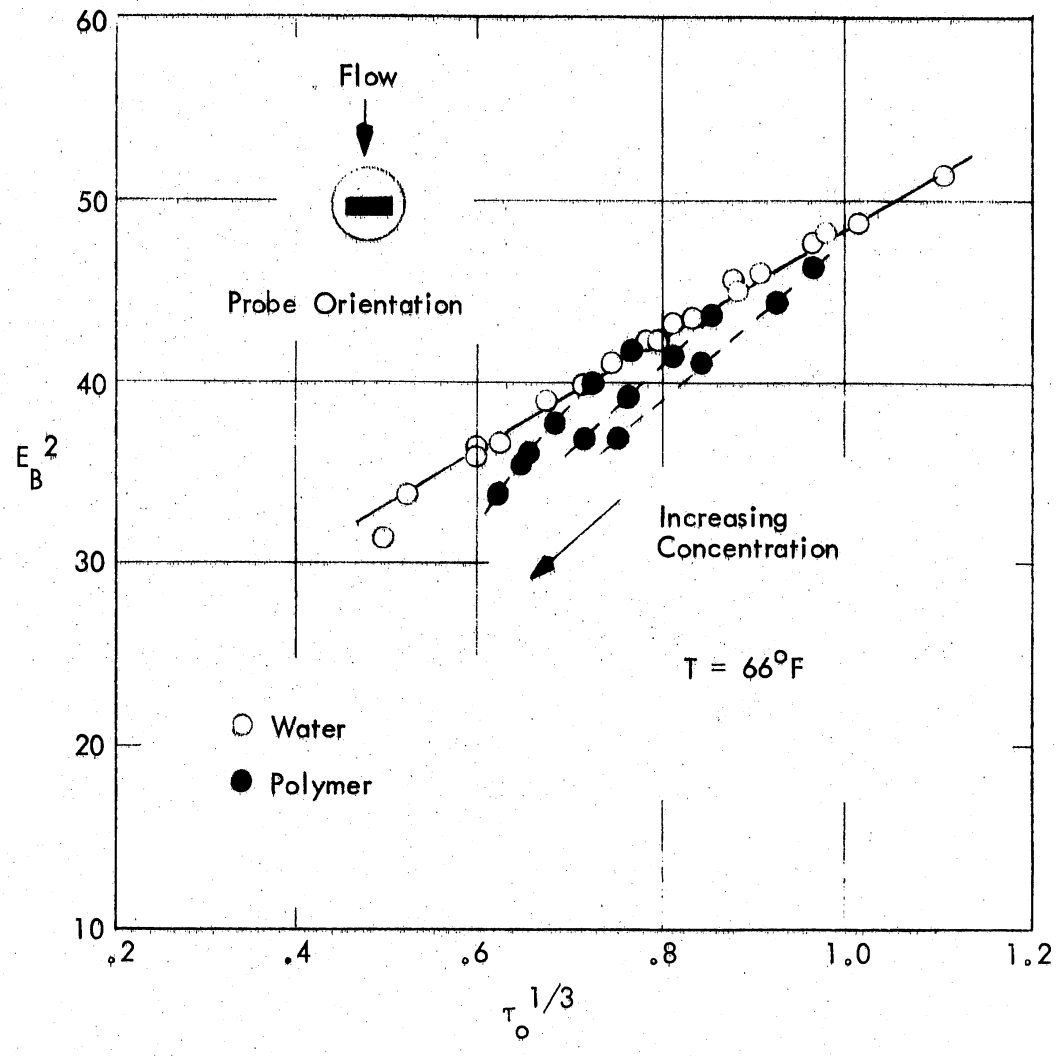

Fig. 25 - Calibration Curve for Flush-Mounted Hot-Film Sensor

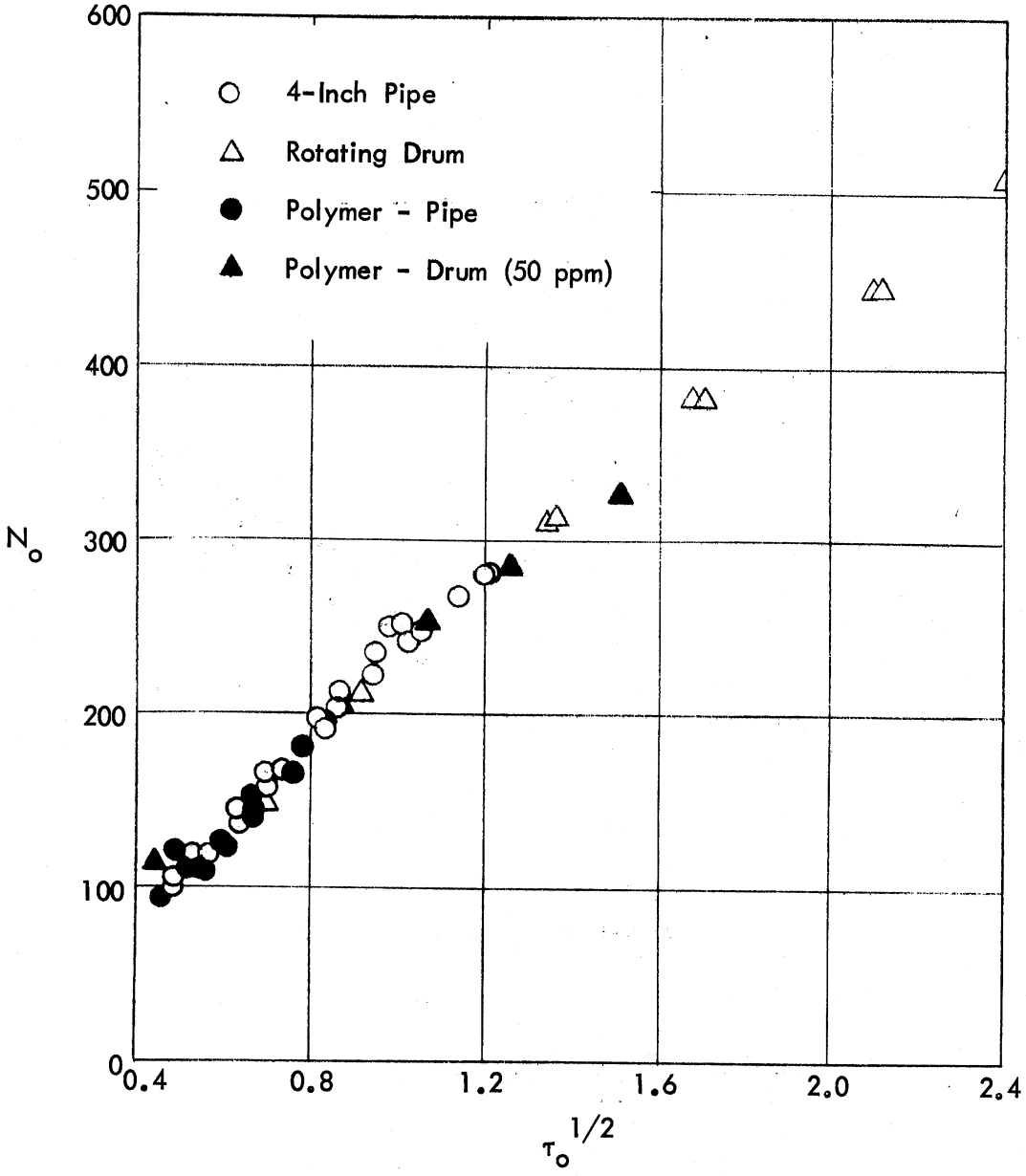

Fig. 26 - Number of Positive-Going Zero Crossings per Second for Various Flows

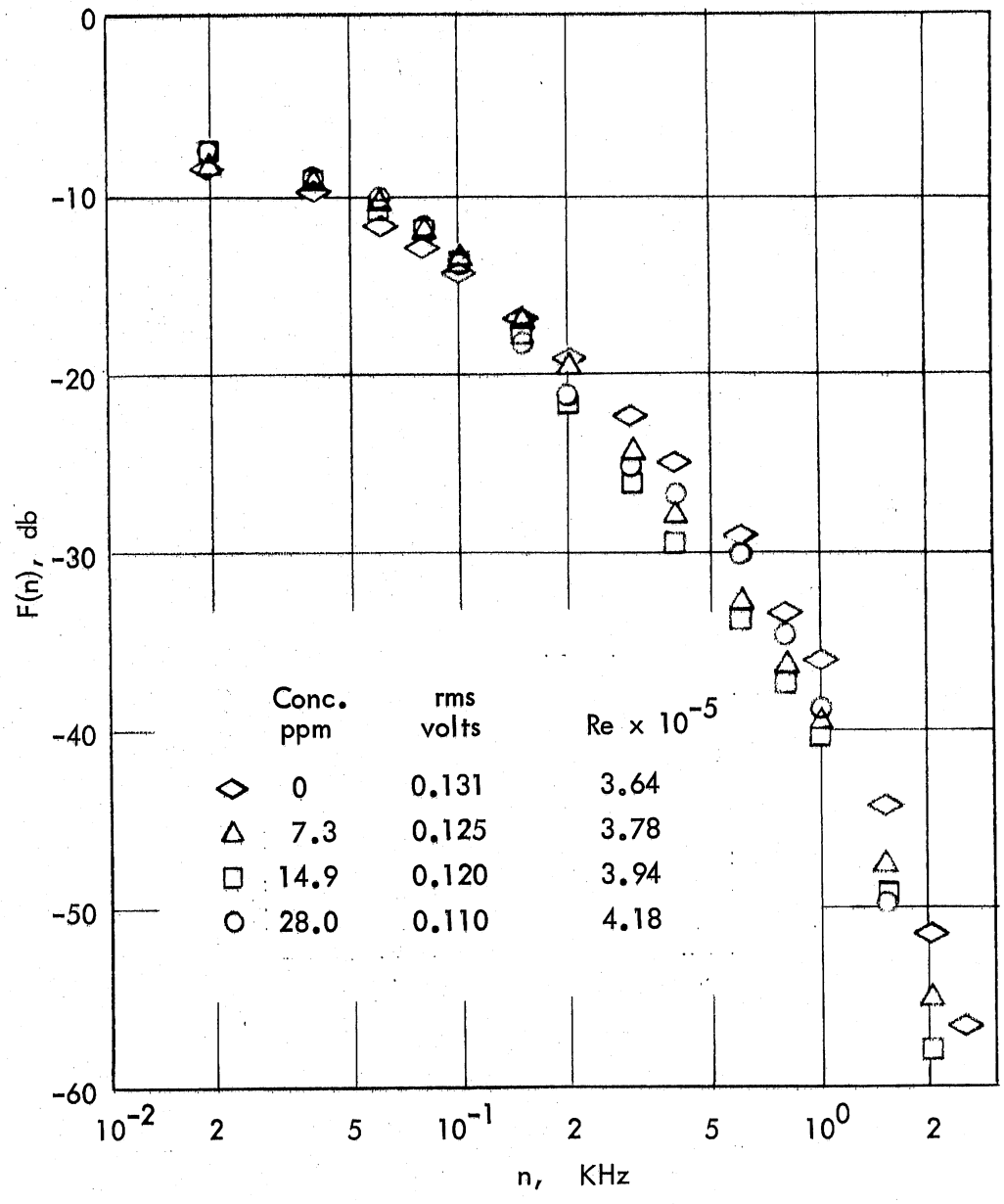

Fig. 27 - Power Spectral Density for Various Polymer Concentrations, 4-Inch Pipe

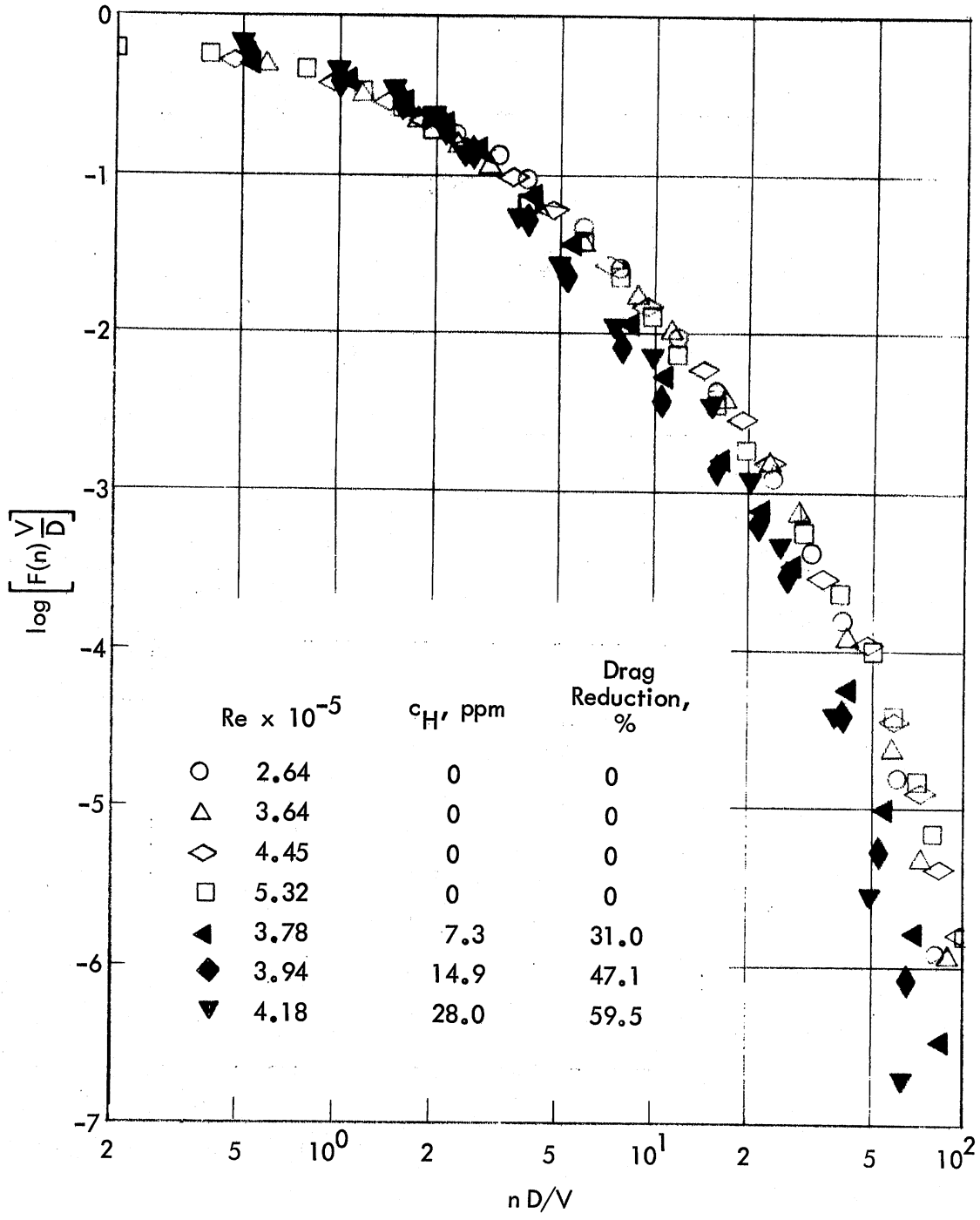

Fig. 28 - Dimensionless Power Spectral Density, 4-Inch Pipe

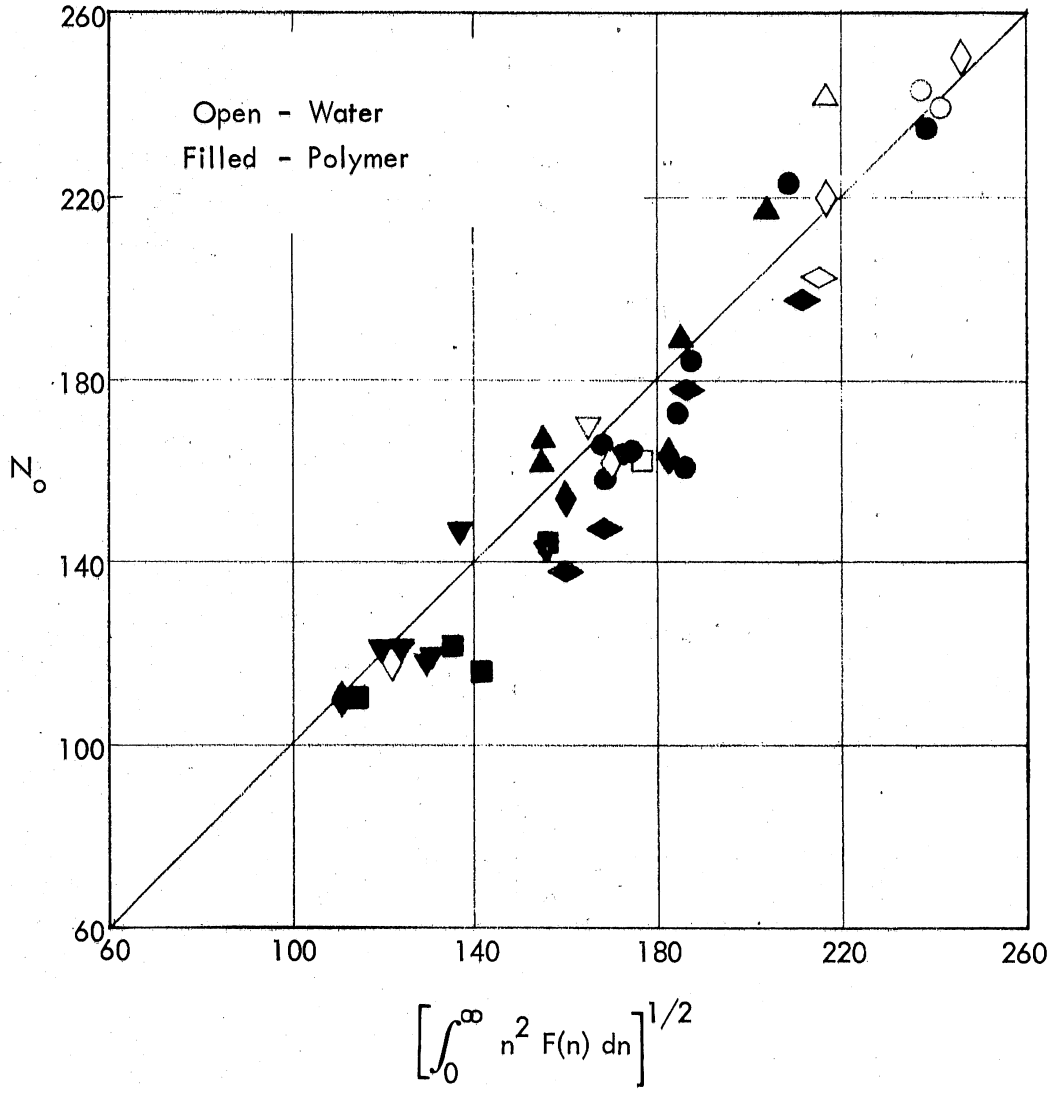

Fig. 29 - Comparison of Measured Zero Crossings and values derived from Frequency Spectra

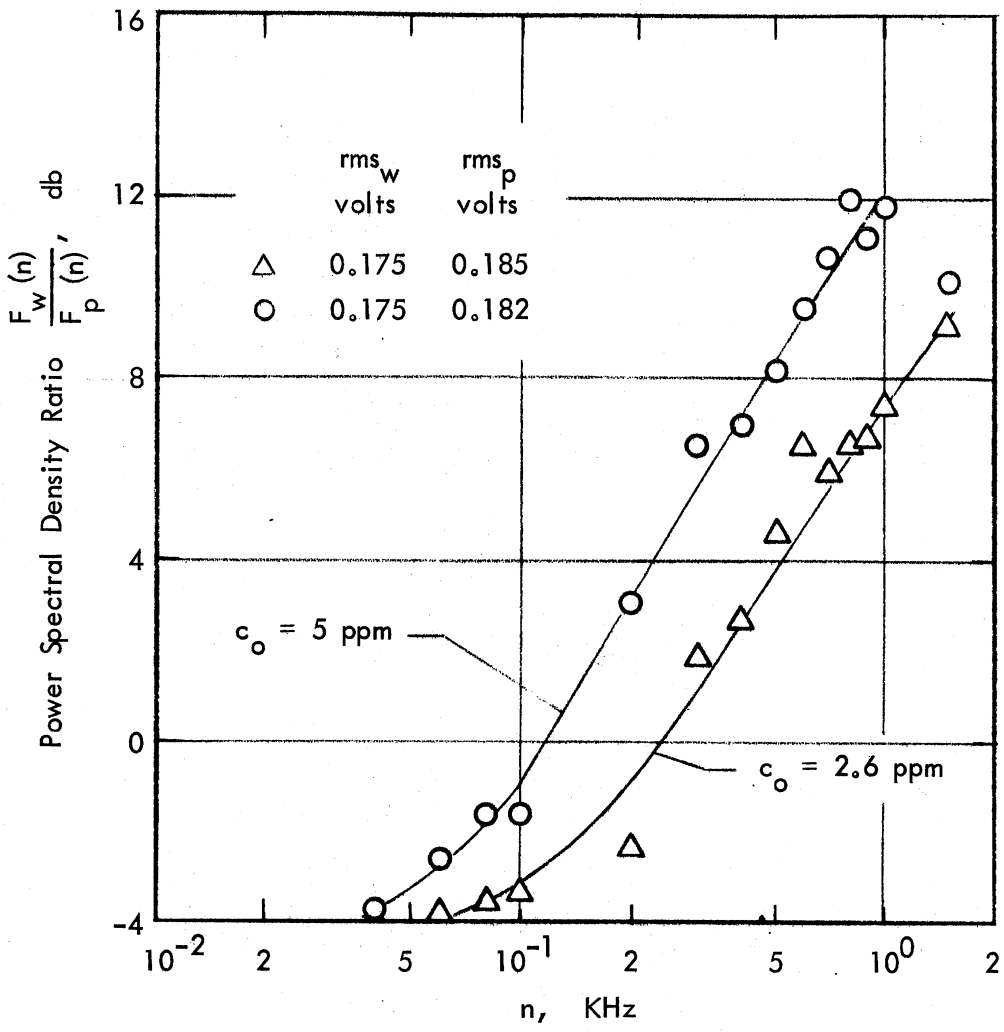

Fig. 30 - Power Spectral Density Ratio, Main Channel

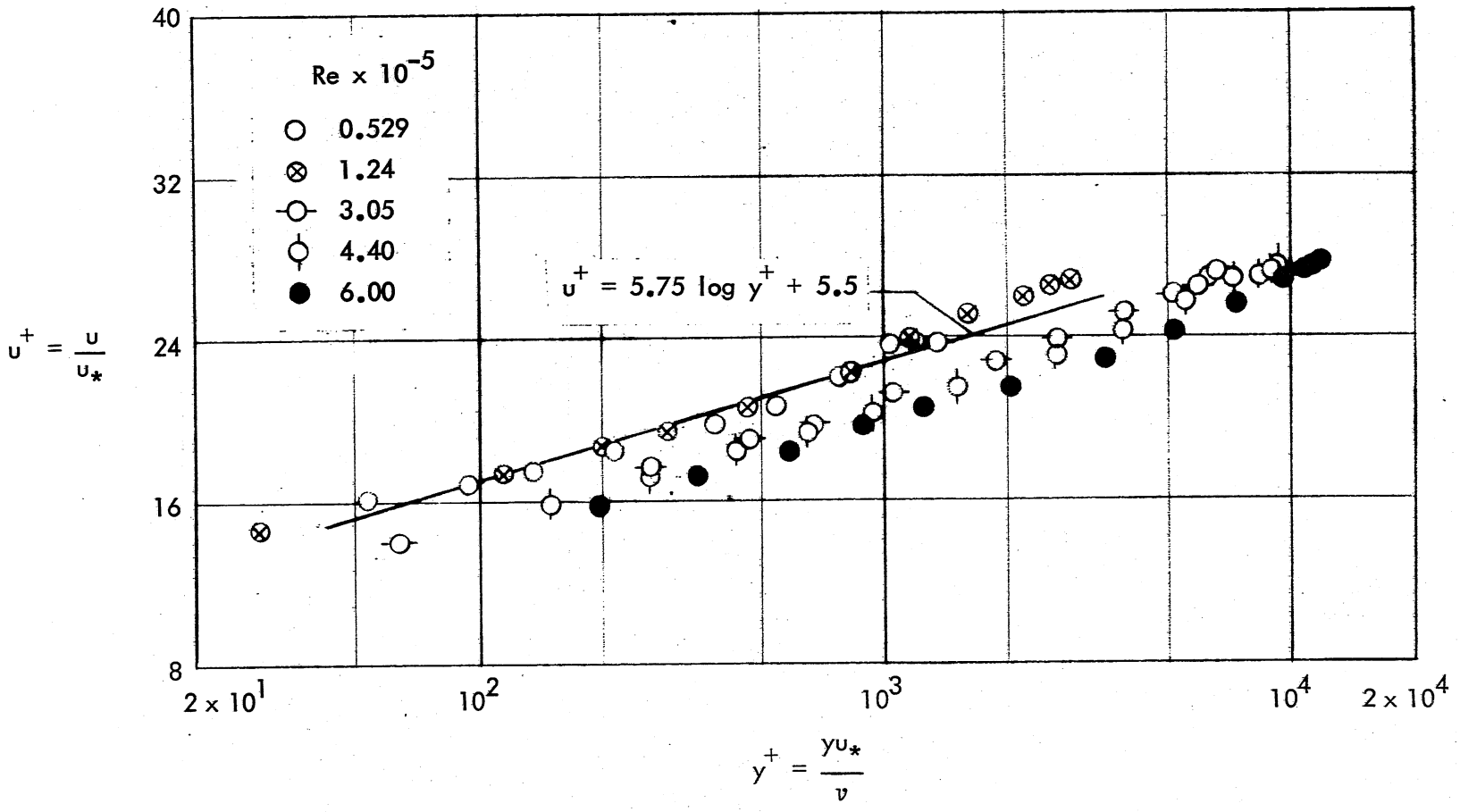

Fig. 31 - Law of the Wall for Water Flows, 4-Inch Pipe

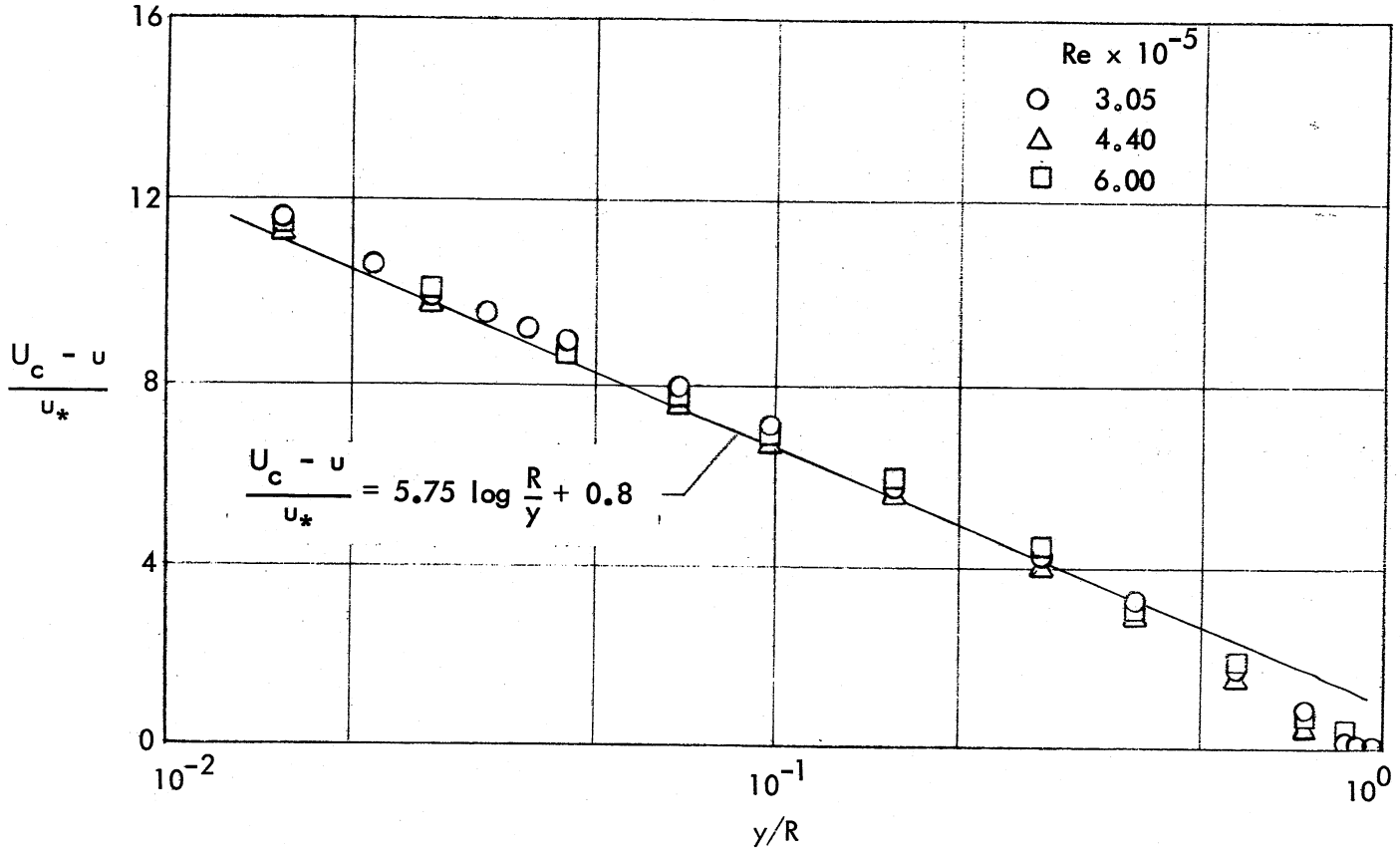

Fig. 32 - Velocity Defect for Water Flow, 4-Inch Pipe

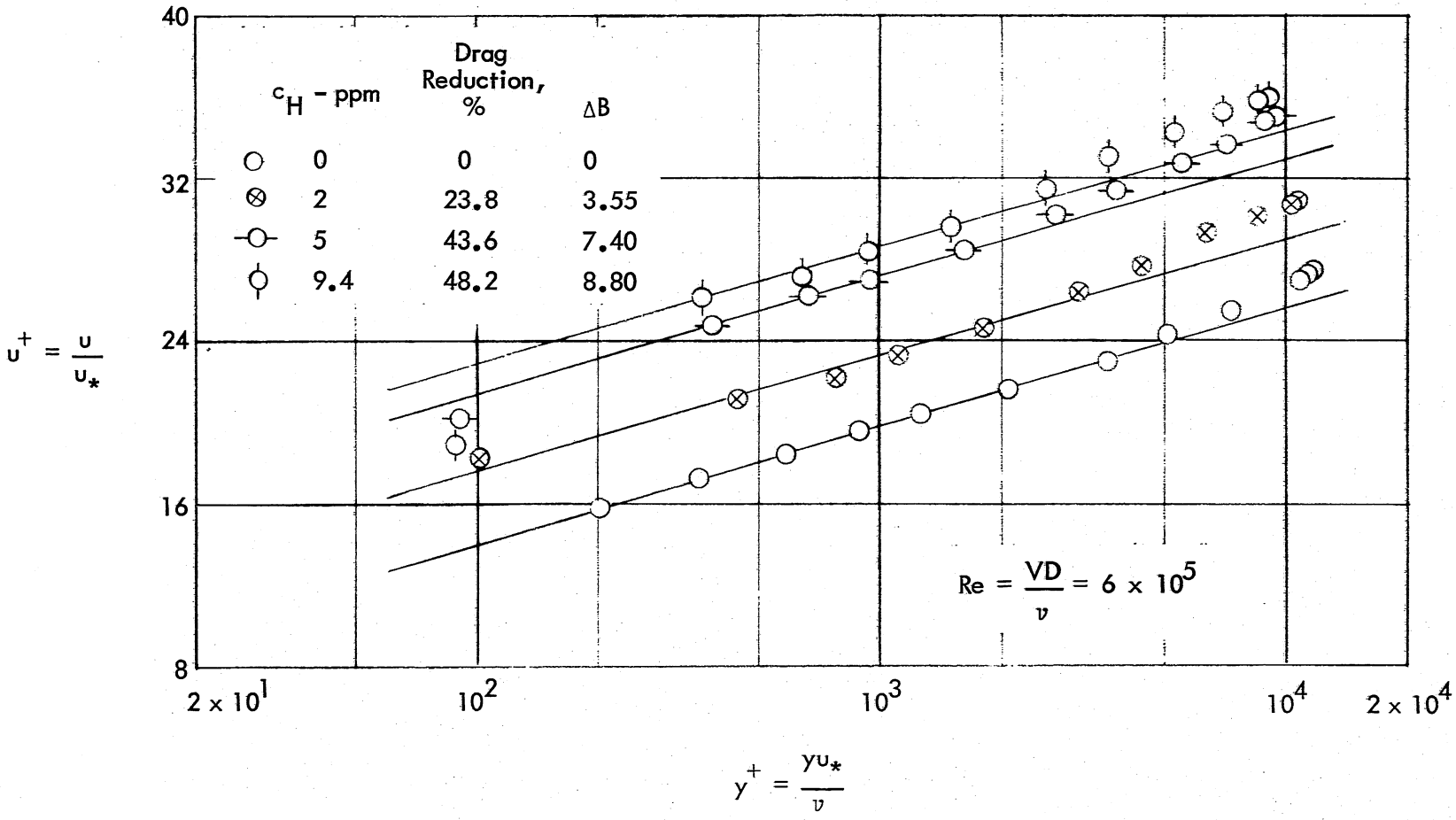

Fig. 33 - Influence of Polymer on Law of the Wall, 4-Inch Pipe

DISTRIBUTION LIST FOR PROJECT REPORT NO. 114

of the St. Anthony Falls Hydraulic Laboratory

Copies	Organization
40	Commander, Naval Ship Research and Development Center, Washington, D.C. 20034, Attn: 38 - Code L41 1 - Code 508 1 - Code 513
2	Commanding Officer, Naval Ship Research and Development Laboratory, Annapolis, Maryland 21402, Attn: 1 - Code A722 1 - Code A824
2	Commanding Officer, Naval Ship Research and Development Laboratory, Panama City, Florida 32401, Attn: Library
11	Commander, Naval Ship Systems Command, Washington, D.C. 20360, Attn: 1 - Code 034 1 - Code 03412 1 - Code 037 1 - Code 037C 1 - Code 08 1 - Code PMS-381 1 - Code 425 2 - Code 205L 1 - Code PMS-393 1 - Code 0371
5	Commander, Naval Ship Engineering Center, Center Building, Prince Georges Center, Hyattsville, Maryland 20782, Attn: 1 - Code 6103 1 - Code 6110 1 - Code 6111 1 - Code 6114D 1 - Code 6136
1	Commanding Officer, Navy Underwater Sound Laboratory, Fort Trumbull, New London, Connecticut 06320
20	Director, Defense Documentation Center, 5010 Duke Street, Alexandria, Virginia 22314
1	Chief of Naval Research, Department of the Navy, Arlington, Virginia 22217, Attn: Mr. Ralph D. Cooper, Code 438
1	Dr. A. Wood, Office of Naval Research Branch Office, 495 Summer Street, Boston, Massachusetts 02210
1	Dr. R. C. Little, Naval Research Laboratory, Washington, D.C. 20390
1	Strategic Systems Projects Office, Department of the Navy, Washington, D.C. 20360

Copies	Organization
3	Officer-in-Charge, Naval Undersea Research and Development Center, 3202 E. Foothill Boulevard, Pasadena, California 91107, Attn: 1 - Code 2501 1 - Code 254 1 - Code 2543
2	Commanding Officer, Navy Underwater Weapons Research and Engineering Station, Newport, Rhode Island 02840, Attn: 1 - J. F. Brady 1 - Library
1	Commander, Naval Undersea Research and Development Center, San Diego, California 92132, Attn: H. V. L. Patrick
1	AFORSR (SREM), 1400 Wilson Boulevard, Arlington, Virginia 22209
1	Library of Congress, Science and Technology Division, Washington, D.C. 20540
2	Commander, Naval Ordnance Systems Command, Washington, D. C. 20360, Attn: 1 - Code 035 1 - Code 054131
1	Prof. J. V. Wehausen, Department of Naval Architecture, College of Engineering, University of California, Berkeley, California 94720
2	California Institute of Technology, 1201 E. California Boulevard, Pasadena, California 91109, Attn: 1 - Dr. A. J. Acosta 1 - Dr. T. Y. Wu
1	Prof. V. Scottron, Hydraulic Research Laboratory, University of Connecticut, Box U-37, Storrs, Connecticut 06268
1	Prof. G. J. Carrier, Harvard University, Pierce Hall, Cambridge, Massachusetts 02138
1	Dr. J. M. Robertson, Theoretical and Applied Mechanics Dept., University of Illinois, College of Engineering, Urbana, Illinois 61801
1	Prof. R. I. Tanner, Brown University, Providence, Rhode Island 02912
3	The University of Iowa, Iowa City, Iowa 52240, Attn: 1 - Dr. H. Rouse 1 - Dr. L. Landweber (Inst. Hydraulic Res.) 1 - Dr. J. Kennedy (Inst. Hydraulic Res.)
1	Dr. A. H. Keil, Department of Naval Architecture and Marine Engineering, Massachusetts Institute of Technology, Cambridge, Massachusetts 02139
1	Dr. T. Francis Ogilvie, Department of Naval Architecture and Marine Engineering, University of Michigan, Ann Arbor, Michigan 48104

Copies	Organization
5	St. Anthony Falls Hydraulic Laboratory, University of Minnesota, Mississippi River at 3rd Avenue S.E., Minneapolis, Minnesota 55414, Attn: 1 - Prof. E. Silberman 1 - Dr. J. M. Killen 1 - Mr. F. Schiebe 1 - Mr. J. M. Wetzel 1 - Prof. J. Ripken
2	U.S. Naval Academy, Annapolis, Maryland 21402, Attn: 1 - Library 1 - Dr. Bruce Johnson
1	U.S. Naval Postgraduate School, Monterey, California 93940, Attn: Dr. T. Sarpkaya
3	The Pennsylvania State University, Ordnance Research Laboratory, University Park, Pennsylvania 16801, Attn: 1 - Director 1 - Prof. John Lumley 1 - Dr. M. Sevik
1	Dr. J. P. Tullis, Colorado State University, Department of Civil Engineering, Fort Collins, Colorado 80521
1	Mr. A. L. Shrier, ESSO Research and Engineering Co., Engineering Technology Department, Florham Park, New Jersey 07932
1	Dr. R. L. Street, Stanford University, Stanford, California 94305
1	Dr. J. P. Breslin, Davidson Laboratory, Stevens Institute of Technology, 711 Hudson Street, Hoboken, New Jersey 07030
2	Hydronautics, Inc., Pindell School Road, Howard County, Laurel, Maryland 20810, Attn: 1 - Mr. P. Eisenberg 1 - Mr. M. Tulin
1	Director, National Science Foundation, Engineering Division, 1800 G Street, N. W., Washington, D. C. 20550
1	Dr. Albert T. Ellis, University of California at San Diego, Department of Applied Mechanics, P.O. Box 109, LaJolla, California 92038
1	Naval Scientific and Technical Intelligence Center, 4301 Suitland Road, Washington, D. C. 20390, Attn: Code 234
1	Mr. N. F. Whitsitt, The Western Company, 2201 N. Waterview Parkway, Richardson, Texas 75080
1	Mr. F. W. Stone, Union Carbide Company, P.O. Box 65, Tarrytown, N.Y. 10591

Copies	Organization
1	Mr. M. Lieberman, ESSO Research and Engineering Company, Government Research Laboratory, P.O. Box 8, Bldg. 8, Linden, New Jersey 07036
1	Maritime Administration, Office of Research and Development, 441 G Street, N. W., Washington, D. C. 20235, Attn: R. Falls, Director
1	Dr. Horance Crawford, Lone Star Gas, Dallas, Texas 75240
1	Mr. W. B. Giles, General Electric Company, R and D Center, Schenectady, N. Y. 12301
1	Prof. A. B. Metzner, Department of Chemical Engineering, University of Delaware, Newark, Delaware 19711
1	Prof. G. K. Patterson, University of Missouri, Department of Chemical Engineering, Rolla, Missouri 65401
1	Mr. J. G. Savins, Mobil Field Research Laboratory, P.O. Box 900, Dallas, Texas 75221
1	Mr. C. S. Wells, LTV Research Center, P.O. Box 6144, Dallas, Texas 75222

Unclassified

Security Classification

DOCUMENT CONTROL DATA - R & D

(Security classification of title, body of abstract and indexing annotation must be entered when the overall report is classified)

1. ORIGINATING ACTIVITY (Corporate author)	2a. REPORT SECURITY CLASSIFICATION
St. Anthony Falls Hydraulic Laboratory University of Minnesota	Unclassified
	2b. GROUP

3. REPORT TITLE

SHEAR AND DIFFUSION IN A LARGE BOUNDARY LAYER INJECTED WITH POLYMER SOLUTION

4. DESCRIPTIVE NOTES *(Type of report and inclusive dates)*

Project Report - May 1968 through November 1969

5. AUTHOR(S) *(First name, middle initial, last name)*

Joseph M. Wetzel
John F. Ripken

6. REPORT DATE	7a. TOTAL NO. OF PAGES	7b. NO. OF REFS
February 1970	70 + ix	18

8a. CONTRACT OR GRANT NO.	9a. ORIGINATOR'S REPORT NUMBER(S)
Nonr 710(71)	Project Report No. 114
b. PROJECT NO.	
SF 35.421.003, Task 1710	
c.	9b. OTHER REPORT NO(S) *(Any other numbers that may be assigned this report)*
d.	

10. DISTRIBUTION STATEMENT

This document is subject to special export controls and each transmittal to foreign governments or foreign nationals must be made only with prior approval of the Naval Ship Research and Development Center, Washington, D. C., 20034.

11. SUPPLEMENTARY NOTES	12. SPONSORING MILITARY ACTIVITY
	Naval Ship Research and Development Center, Washington, D. C. 20034

13. ABSTRACT

Experimental studies involving velocity profile measurements and polymer diffusion measurements were made in a plane boundary layer with length varying up to 40 ft, thickness varying up to 15 inches, and Reynolds number varying up to 8×10^7. Aqueous solutions of Polyox WSR-301 of 250 to 2000 ppm were injected tangentially at the boundary near the origin of a boundary layer having a stream velocity of 18 fps.

Diffusion of the polymer from the boundary up into the boundary layer was evaluated from profiles made by sampling with withdrawal tubes located at various stations along the flow axis. A fluorescent marker dye was used for the evaluation.

Velocity measurements served to define the profile and permitted profile extrapolation to the boundary for boundary shear evaluations.

The maximum drag reduction of 35 per cent over a 40-ft boundary length exposed to V = 18 fps occurred with an injection of 0.004 lb/sec of polymer per foot width, which resulted in a downstream wall concentration of about 30 ppm.

A flush-mounted hot-film sensor was calibrated for both water and polymer flows in a gravity-flow pipe facility. The calibration curve was influenced by the addition of polymer. Measurements of the zero crossings and frequency spectra of the turbulent fluctuations, as well as velocity profiles, were made for various polymer concentrations in the commercially rough pipe. Zero crossings were found to correlate with the square root of the wall shear stress.

14. KEY WORDS	LINK A		LINK B		LINK C	
	ROLE	WT	ROLE	WT	ROLE	WT
Drag reduction						
Polymer solutions - injection						
Turbulent boundary layer						